Making negatives and plates for printing by electroerosion: I. Physical principles

by M. S. Cohen
K. S. Pennington

Electroerosion printing involves removal of the aluminum overlayer from selected areas of a black-coated paper. "Direct negatives" as well as "direct plates" for use in offset lithographic printing may also be generated by electroerosion if a clear polymer sheet is used as the substrate instead of paper, and the black base layer is omitted. If such a substrate is metallized and written by electroerosion, the desired direct negative is created in principle since the metal stops transmitted light and the polyester does not. The direct plate is simultaneously created in principle since the aluminum is hydrophilic and the polyester is hydrophobic. Practical realization of these concepts required studies of the physical principles of the processes involved, which led to techniques for avoidance of mechanical scratching of the aluminum film during writing. For this purpose a mechanically hard underlayer was applied to the substrate under the aluminum, while a very thin lubricating overlayer having some electrical conductivity was applied over the aluminum. The underlayer consisted of silica particles in an organic binder, while the overlayer consisted of graphite particles in a binder. Although scratching is less for smooth than for rough underlayers, rough underlayers were preferred because they offered better writing reproducibility. In particular, debris created during writing was scoured away from the styli in rough-underlayer samples. For writing, a two-phase driver was used, in which the first phase provided a high current for Joule heating with consequent breaking of direct local aluminum–stylus contacts, while the second phase provided an arc which removed the remainder of the aluminum under the stylus.

1. Introduction

Much of the world's printing industry is based on offset photolithography. This technique uses a "plate" or "master" on which the information to be printed has been transcribed as hydrophobic regions in the initially uniformly hydrophilic surface (**Figure 1**). After processing, the plate is wrapped around a rotating "plate cylinder" arranged so that the plate surface is continuously coated with both oil-based ink and water from separate sources. The ink adheres preferentially to those areas of the plate which previously have been made hydrophobic and not to the water-receptive hydrophilic background. During press operation, ink from the plate is transferred first to a rubberized "blanket cylinder" and then to the paper.

Preparing the printing plate usually involves several chemical and physical processes, skilled operators, and appreciable time. For example, the traditional method first requires manual cutting and positioning of the "camera copy" to be printed, followed by production of a "photonegative" by photographing the copy with a special copy camera. The photonegative is then usually developed using wet-chemical processing. The developed photonegative is used to make a contact exposure of a blank plate in a special "plate-making" machine. Such blank plates have been photosensitized and treated during manufacture in such a way that after proper exposure and development the surface of the plate is rendered hydrophobic and hydrophilic respectively in areas corresponding to the desired ink-retaining and ink-rejecting regions. Although some shortcuts in this procedure have been developed, the process remains slow and expensive and involves wet-chemical development.

Considerable improvement in these techniques is possible through the use of modern computers for formatting the copy, together with special computer-output hard-copy technologies. The information to be printed, including text, line drawings, and even halftone pictures, can be entered into a computer system, edited and merged at a computer terminal by an operator, and stored in computer memory. If a high-resolution, hard-copy computer-output device is available, the operator can then immediately obtain camera-ready copy, enabling preparation of a photonegative using a standard copy camera. A common example of such a device is a computer-driven photocomposer; here the computer output appears on the face of a CRT which is photographed to yield hard copy.

Recently an alternative high-resolution computer-output device, the IBM 4250 printer, has been developed[1] using the principle of electroerosion. By using the electroerosion paper designed for use with this printer, camera-ready copy can be prepared faster and at lower cost with this device than with a conventional photocomposer, since no photographic steps are employed.

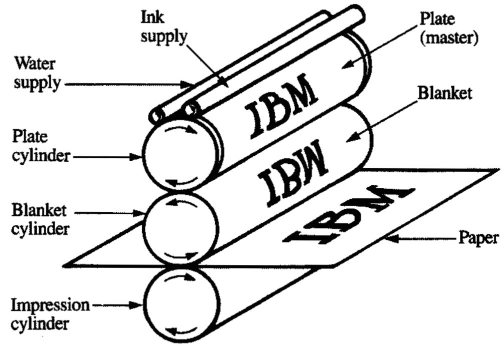

Figure 1

Principles of offset lithography. Water and oil-based ink are supplied by "fountains" to the plate, which is wrapped around the rotating plate cylinder. The ink is then transferred to the rubberized blanket cylinder, and from the blanket cylinder to the paper.

Electroerosion paper consists of a paper base coated first with a black organic underlayer and then with a thin, white-appearing overlayer. The overlayer is removed during writing to reveal the black underlayer. Early "electrosensitive" papers had overlayers consisting of white conductive or semiconductive pigments in a binder [1]; recent electroerosion materials [1–3], e.g., for the IBM 4250 printer, use a thin vacuum-deposited aluminum layer over the black organic underlayer (**Figure 2**). This paper is concerned solely with the latter type of material. Multiple styli, typically tungsten wire, are set in a head, which sweeps across the page while maintaining good electrical contact between the styli tips and the aluminum overlayer. An electric pulse is applied to the appropriate stylus at the correct time to cause writing. An electric arc is thereby created, causing local removal of the aluminum by disintegration, e.g., vaporization, thereby exposing the underlying black layer so that optical contrast with the surrounding aluminized surface is provided. A variety of different electroerosion papers have been developed using various blackening agents in the underlayer, as well as roughening agents to give the surface a pleasing matte appearance [2–6].

In the past, low-resolution electroerosion printing has been used in instrumentation recorders as well as in computer hard-copy output devices which generated

[1] Information Products Division, IBM Böblingen, Germany. The device writes with a center-to-center spacing of 42.3 μm, using 32 tungsten styli of 80-μm diameter in the head. See K. S. Pennington, "Making Negatives and Plates for Printing by Electroerosion: Introduction and Overview, *IBM Journal of Research and Development*, this issue.

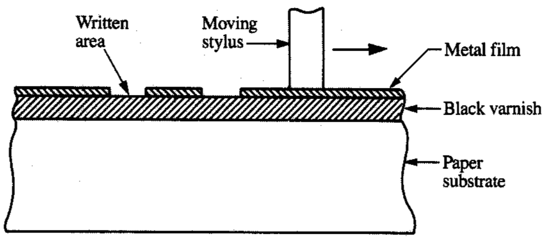

Figure 2

Principles of electroerosion printing on conventional electroerosion paper. Current pulses are applied to the appropriate styli of a moving writing head. These pulses creates arcs which locally erode away the metal film covering an underlayer of black "varnish" material. (Not to scale.)

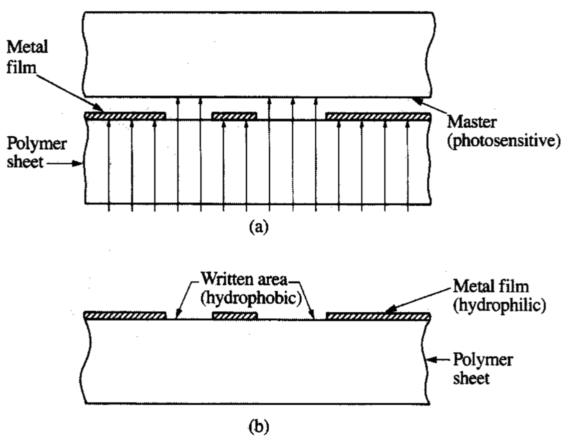

Figure 3

(a) Use of electroerosion writing to produce a direct negative for immediate contact exposure of a conventional photosensitive plate in a plate-making machine. Here light (arrows) can pass through areas which were previously electroeroded away, but is blocked in uneroded areas. (b) Use of electroerosion printing to produce a direct plate for immediate use in an offset lithography press. Here the metal layer is hydrophilic, so it accepts water from the water fountain on the press, while the underlayer which is locally exposed by electroerosion is hydrophobic, so it accepts ink from the ink fountain on the press. (Not to scale.)

graphics as well as text. However, it was only with the advent of the IBM 4250 printer that high-resolution electroerosion printing made possible an alternative to the conventional computer-driven photocomposer for producing camera-ready copy for offset printing. While this is recognized as a most useful achievement, it is the purpose of this series of papers to point out that the electroerosion writing technology can provide simplifications in offset-plate production well beyond furnishing camera-ready copy.

- *Direct negative*

Through the use of special direct-negative/direct-plate (DNP) sheet material, electroerosion printing technology can be used to create negatives directly. In principle, a DNP material can be made by depositing aluminum film on a transparent substrate. Subsequent electroerosion writing results in opaque and transparent regions corresponding to the unwritten and written areas, respectively [**Figure 3(a)**]. Such a sheet then can be used immediately in a plate-making machine to make a plate by contact exposure; i.e., the electroerosion printer has made a *direct* negative.

- *Direct plate*

Further simplification of the plate-making process can be achieved if the electroerosion printer is used to produce a plate directly, i.e., if the output of the printer is used in a printing press immediately, without any intermediate steps. Several authors have suggested that electroerosion technology could in fact be extended to provide such a *direct* plate [7, 8]. The basic structure of a DNP material required for this purpose is shown in principle in **Figure 3(b)**. This structure is identical to that of the direct negative [Figure 3(a)], but now the aluminum layer is assumed to be hydrophilic, while the underlying polymer substrate is hydrophobic. Thus the electroerosion written regions, from which aluminum is removed, become hydrophobic and accept ink, while the unwritten regions do not. A short-run direct plate is thus produced, since the information to be printed has been successfully mapped onto the plate in terms of its surface affinity.

- *Approach of present work*

The initial feasibility of the direct-negative and direct-plate concept was demonstrated some years ago,[2] but difficult practical problems were encountered. It was found that when a multistylus writing head is used, such problems as scratching, head fouling, and degradation of writing quality must be overcome. (To help prevent possible confusion between electroerosion processes and offset-printing processes, the former processes are hereafter designated as "writing" rather than printing.) A study of the physics and chemistry of the electroerosion writing process was carried out in order to address these problems.

Although full rolls of DNP material were needed for practical use with the IBM 4250 printer, it was found

[2] J. G. Cahill, P. S. Hauge, and K. S. Pennington, IBM Thomas J. Watson Research Center, Yorktown Heights, NY, 1980, private communication.

convenient to carry out the exploratory work on small (5 × 5-cm) samples coated on suitable polymer substrates. For this purpose organic film coatings were made either with a photoresist spin coater or by cutting from somewhat larger samples made with hand "draw-down" techniques. The metal films were deposited in a standard laboratory vacuum system. The resulting samples were tested on a specially modified electroerosion writing system which used the electronics of a prototype of the IBM 4250 printer, and which had a writing head of 14 styli, each of 80-μm diameter. The sample was placed on a soft sponge-rubber backing and secured by the application of vacuum; the head was moved across the sample in individual sweeps during writing experiments. Examination of these samples was carried out by means of optical and electron microscopy and with other instruments described below.

Studies carried out by these means provided the physical foundations for the design of practical materials, and are described in this paper. A detailed discussion of the fabrication techniques and tests involved in *large-scale* practical fabrication of DNP material is given in Part II of this series of papers, while Part III is concerned with the use of DNP material as a direct negative and direct plate. The IBM DNP material sold under the trade name "electroNEG" for use with the IBM 4250 printer is largely based on the studies described in these papers.

2. The scratching problem

Early studies of the direct plate and direct negative were carried out on metallized polyester sheets (Figure 3) using a single-stylus writing head with careful control of the force of the head on the substrate.[3] Under these conditions, workable direct negatives and direct plates were obtained. However, unsatisfactory quality was obtained with the prototype of the IBM 4250 printer, because that printer employed a multistylus head which did not permit adjustment for minimization of the force on individual styli. Under these conditions, severe scratching of the substrate resulted (**Figure 4**). This scratching was mechanical in nature and was unrelated to the writing process, as was substantiated by the observation that scratching occurred if the head was swept with the write power off. Such scratching results in unwanted local light transmission when the written sheet is used for a direct negative, and unwanted local inking when the sheet is used for a direct plate.

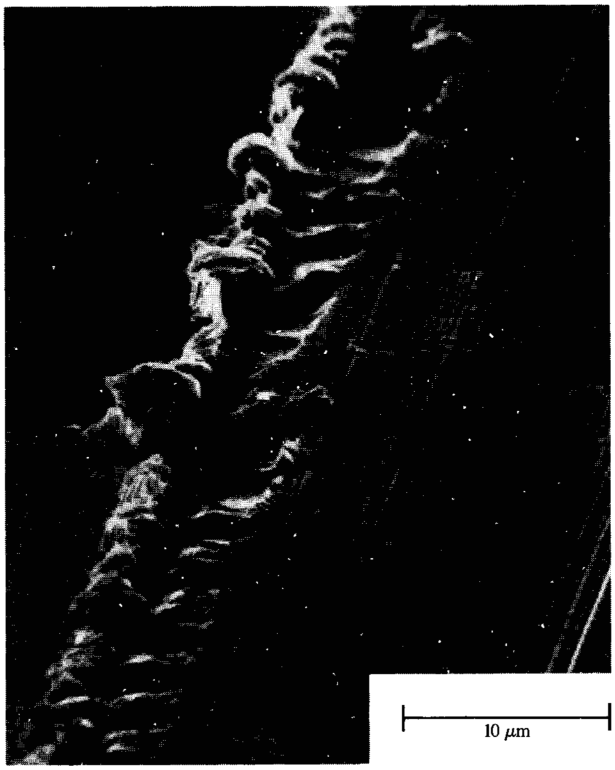

Figure 4

Scanning electron micrograph of a scratch created by electroerosion writing on the surface of a commercial aluminized polyester sheet.

- *Mechanisms of scratching*

The scratching observed in metallized polymer sheets was initially incorrectly interpreted as simple adhesion failure between the metal film and the underlying substrate. Because it is of great technological interest, the adhesion of a metal film to its underlying substrate has been studied by many workers [9–13]. A proposed quantitative test for such adhesion strength involves moving a loaded stylus over the surface of the metal film [9]; the conditions of this test are thus very similar to those involved in electroerosion writing. The test, which has been applied to both glass [9] and polymeric [10] substrates, consists first of determining that stylus loading which causes the onset of scratching, and then relating this loading to the adhesive strength. In particular (see the Appendix), it was noted that a properly loaded, spherically tipped stylus of radius r (**Figure 5**) causes plastic deformation in the substrate according to

$$P = W/\pi a^2, \qquad (1)$$

where P is the hardness in the plastic-flow region (the average pressure on a spherically tipped indenter), W is the force on the stylus, and a is the radius of the circle limiting the stylus–substrate interface. The shear force F on the film is then shown to be

$$F = aP/(r^2 - a^2)^{1/2}. \qquad (2)$$

[3] See footnote 2.

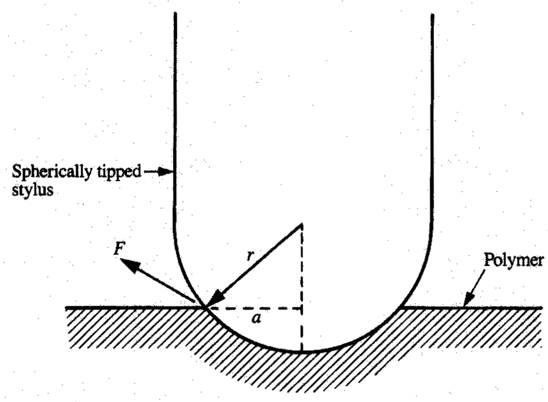

Figure 5

Spherically tipped metal stylus pressed under force W into a polymer. The stylus radius is r, while a is the radius of the indentation. A tangential shear force F is developed.

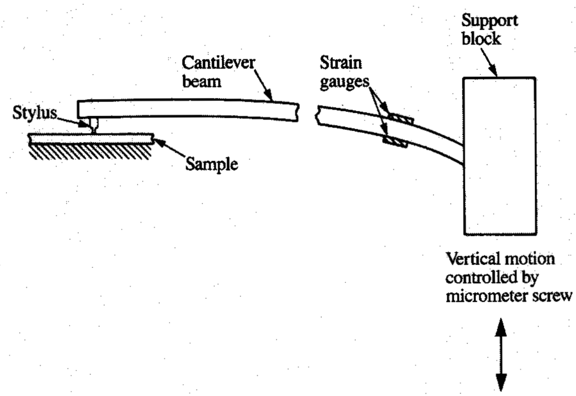

Figure 6

Construction of the scratch tester. A metal stylus is fastened to the end of a cantilevered aluminum beam. The fixed end of the beam is moved by means of a precision micrometer screw, while the resulting strain is measured by strain gauges fastened to the top and bottom of the beam. The outputs of the strain gauges are fed into a bridge circuit connected to an amplifier. The sample is held on a stage which can be translated horizontally by a motor. (Not to scale.)

These relations give F as the adhesion shear strength if W is taken as the threshold loading at which scratching starts.

This adhesion test has been criticized on the grounds that the scratching mechanism is far more complex than is represented by this simple adhesion-failure model [11]. The scratching phenomena studied in the present work have also exhibited appreciable complexity, so that the simple adhesion-failure mechanism must be rejected. It is seen in Figure 4, for example, that very considerable destruction of the substrate is involved in the scratching of metallized polymers. When such damage occurs in the underlying polymer, the overlying metal film disintegrates because its tensile strength is greatly exceeded.[4]

The observed destruction of the underlying polymer can be attributed to either of two different mechanisms [13]:

1. Adhesive wear, where the stylus cold-welds to the overlying metal film. Because of the resulting strong film–substrate bond, shear then takes place deep in the underlying polymer.
2. Plowing, where the polymer is cut directly by asperities at the bottom of the stylus.

• *Scratch-reduction methods*

The polymer substrate material used most widely in this study was polyester.[5] However, many other aluminized polymer sheets were studied, including polycarbonate, polysulfone, polyimide, nylon, ionomer, and polypropylene. They all showed the unacceptable scratching characteristics exhibited by aluminized polyester.

In order to provide a quantitative measure of scratching, a special scratch tester was constructed. The tester was similar to those proposed for testing thin-film adhesion [9–13]; i.e., a loaded stylus was moved across the sample, and scratching was observed as a function of stylus loading. In the present case [14], the tungsten stylus was fixed to one end of a cantilever beam whose other end was fastened to a support which could be adjusted in vertical position, thereby bending the beam and hence permitting adjustment of the stylus loading (**Figure 6**). The strain in the beam was measured by the output of a bridge circuit containing a pair of strain gauges mounted on opposite sides of the beam; by precalibration with known forces, this output was translated directly into stylus loading. In operation, a series of parallel tracks was made, each with a specified loading ranging from about 1 to 10 g (force from about 10 to 100 mN). For a quantitative measurement of the extent of the scratching, the optical transmission of track segments was measured in a microscope with the aid of a photodiode, using chopped light and a phase-sensitive detector.

Measurements made with this apparatus confirmed the unacceptability of simple metallized polymer sheets for the

[4] Disintegration of the metal film was found even when an elastomer such as a polyurethane was used as the substrate. In this case the elastic limit of the substrate was not exceeded, and no permanent deformation as observed in Figure 4 was seen, but the aluminum film was unacceptably crazed in the track of the stylus because its tensile strength was exceeded.

[5] Polyethylene terephthalate, trade name Mylar®, E. I. du Pont de Nemours & Co., Wilmington, DE.

present application. However, as described in detail below, further work showed that scratching can be significantly reduced if the structure is modified to include appropriate layers both under and over the aluminum film.

Underlayer

Since the scratching of metallized polymer sheets originates largely in the destruction of the polymer underlying the metal film by one of the two mechanisms listed previously, it should be advantageous to use a harder substrate. However, considerable flexibility of the polymer sheet is required for ensuring good electrical contact with all the styli of the head as well as for permitting handling of the material in roll form; the polymer underlayer therefore cannot be hard throughout its thickness. In order to meet both the compliance and hardness requirements, a multilayer approach was chosen in which a thin, hard underlayer was coated on a flexible polymer sheet prior to the metallization step. A typical structure consisted of a polyester sheet about 50 to 100 μm thick, on which a hard underlayer of 5 to 10 μm had been coated; an aluminum film some tens of nm thick was then vacuum-deposited on the underlayer.

Two types of hard underlayers were studied, both of which showed improved scratch resistance:

1. Smooth, hard polymers consisting, for example, of highly cross-linked silicone resins [15–17].
2. Hard particles embedded in a suitable binder, e.g., silica in a cross-linked cellulosic binder, typically cellulose acetate butyrate (CAB).[6] (See Part II for details of the sample-preparation techniques.)

The deformation exhibited by simple metallized polymer sheets (Figure 4) is clearly reduced by the inclusion of an underlayer of smooth, highly cross-linked silicone resins[7] (**Figure 7**); the scratching is correspondingly minimized. (However, as pointed out below, further investigation showed certain disadvantages of smooth underlayers.) Alternatively, an underlayer of hard particulate matter in a suitable binder gives a rough underlayer which also shows little deformation. However, because the local stylus pressure on the peaks of such a structure is very high, some localized scratching occurs in the stylus tracks. A typical transmission micrograph of such a sample, having an underlayer of silica particles in a cellulosic binder, is shown in **Figure 8**. With the aid of the scratch tester and the optical transmission apparatus described above, curves of percentage light transmission vs. stylus loading were obtained. As illustrated in the curve of **Figure 9**, the light transmission is directly proportional to loading, so that the slope of such curves represents a figure of merit for a

[6] Cellulose acetate butyrate 553-0.4, Eastman Chemical Products, Kingsport, TN.
[7] Silicone Hard Coating Resin SHC 1010, General Electric Co., Waterford, NY.

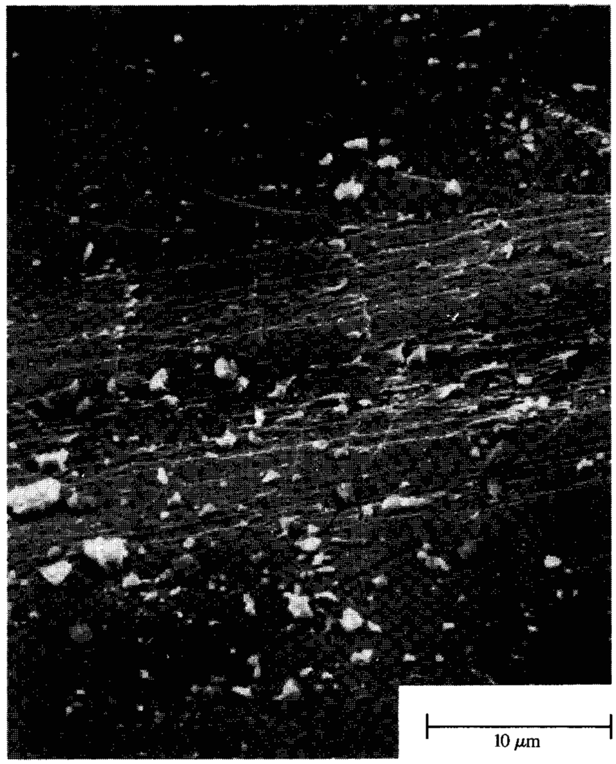

Figure 7

Reduction in scratching when a smooth, hard underlayer is coated on the polymer sheet before metallization. Here a 1.9-μm-thick film of highly cross-linked silicone resin was applied to a polycarbonate substrate. Compare with Figure 4.

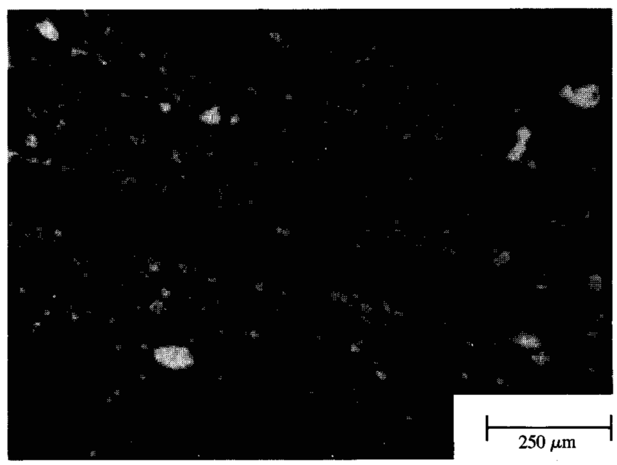

Figure 8

Transmission optical micrograph of scratched region of sample with underlayer of silica in cellulosic binder. The average silica particle size was 3 μm, while the PVC was 7.6%. A 50-nm aluminum film was vacuum-deposited on the underlayer. (There was no overlayer.)

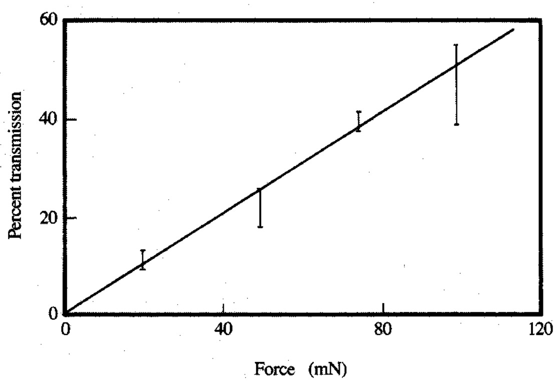

Figure 9

Optical transmission through scratched area vs. stylus force for the sample of Figure 8. A 75-μm-diameter tungsten stylus was used in the scratch tester.

Table 1 Dependence of scratching on silica in underlayer.

SiO_2 loading by weight (%)	*SiO_2 particle size* (μm)	*Slope* (%/mN)
13	4.5	0.111
13	3.0	0.051
13	0.6	0.012
20	0.6	0.026
13	0.6	0.012

given structure. Values of such slopes for a variety of compositions are given in **Table 1**. Here it is seen that lower slopes are obtained if the underlayer is rendered smoother either by reducing the silica particle size for a given silica loading, or by reducing the silica loading for a given particle size. It was also found that the slope could be reduced by calendering after coating the underlayer (see Part II).

While incorporation of the hard underlayer significantly suppressed the scratching, it still did not reduce it to acceptable limits.

Overlayer

The classical adhesive-wear mechanism (stylus cold-welding, sublayer shear) was cited above as one of two possible phenomena involved in scratching. If adhesive wear is in fact the predominant mechanism associated with scratching, the application of lubricants over the metal layer should reduce scratching, since the shear is then harmlessly confined to the lubricant layer.

Several lubricants were tried. Among the most successful were long-chain fatty acids, e.g., lauric, stearic, and arachidic acids [13], and silicone oils [18]. It was found that application of these lubricants did indeed result in decreased scratching even on simple aluminized polymer sheets, indicating that the scratching may be associated more with adhesive wear rather than plowing. However, application of a lubricant *alone* did not result in acceptable scratch resistance.

On the other hand, application of the lubricants just described *combined* with the use of a hard underlayer gave scratch resistance greater than obtained with either measure alone. In spite of this improvement, however, such "boundary-layer" lubrication [13] still gives insufficient protection at local areas of high stylus pressure, e.g., at peaks in rough-underlayer structures. A thicker lubricant or protective layer is therefore required. However, for ease of handling, such a thick layer should be solid rather than liquid; it should provide adequate conductivity in order not to inhibit the writing process (see Section 4); and upon writing it should disintegrate easily without creating debris which could foul the writing head (Section 5). A good candidate for this kind of overlayer is a film containing laminar-structured (lubricating) particles in a suitable binder. Graphite in cellulosic binders has received the most attention in the present work; such materials are commercially available as dispersions in various solvents.[8] Other laminar-structured particles having some electrical conductivity may be considered [19]; in the present study MoS_2 showed good lubrication but was rejected because of odor generation during writing. (Noxious gases were apparently created by the high-temperature arc during writing.)

The binders in the commercially available graphite-containing lubricant products are often cellulosic in nature, with a graphite/binder ratio about 4 : 1 or higher. The graphite/binder ratio of these materials was decreased by the addition of more binder material, usually CAB. A higher binder content imparts greater strength to the overlayer and inhibits smudging during handling, while producing certain changes in electrical characteristics (see the subsection on results of writing studies); however, increased organic binder content also contributes to fouling (see Part II). Formulations were also made in which the binder was cross-linked to form a thermoset polymer (see Part II).

3. Smooth-underlayer samples

As was pointed out previously, scratching associated with the peaks of a hard, rough underlayer can be reduced if

[8] Acheson Colloids Co., Port Huron, MI.

the roughness is decreased, e.g., by decreasing the particle loading (Table 1). In the limit, the hard particles can be eliminated entirely, giving a completely smooth underlayer. By fabrication with highly cross-linked polymers, this underlayer can be made as hard as required for suppression of underlayer wear. Samples made with underlayers of highly cross-linked silicone resins (Figure 7) or with polyurethanes made by cross-linking cellulosic resins with isocyanate thus exhibited very little scratching, particularly when the aluminum layer was overcoated with a graphite-containing overlayer as previously described.

Unfortunately, while such smooth structures showed little scratching on the scratch tester, very poor writing resulted when the electroerosion apparatus was tested. Under these circumstances the written area was very much smaller than the stylus contact area, and often no material at all was removed as a result of energizing the styli. In contrast, fairly good writing was observed with samples having a rough, hard underlayer, or with smooth samples having a soft underlayer, e.g., aluminum directly on polyester, even though the latter samples typically exhibited considerable scratching. This difference in writing behavior between smooth and rough samples originates in the difference in ability of the electronic

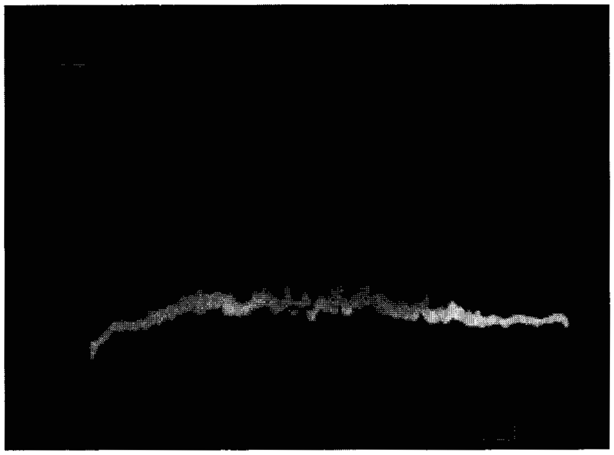

(a)

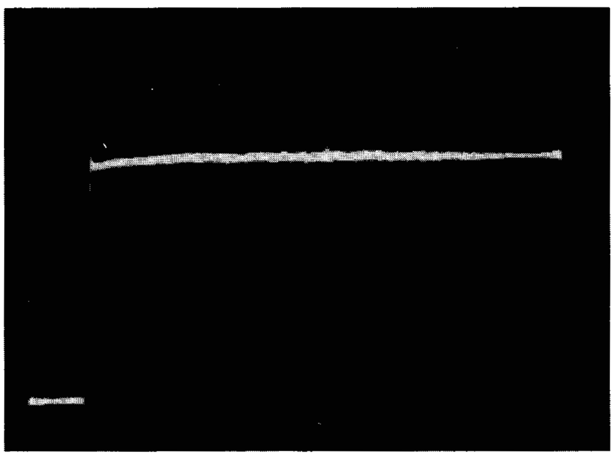

(b)

Figure 10

Writing waveforms for sample consisting of 50 nm of aluminum with thin overlayer of graphite in binder; underlayer was smooth cross-linked CAB. Dissipated power was insufficient to write (remove aluminum). Single-phase driver used with 200-Ω internal impedance at –100 V output. (a) Voltage across sample; 2 V per vertical division, 5 μs per horizontal division. (b) Current through sample; 50 mA per vertical division, 5 μs per horizontal division.

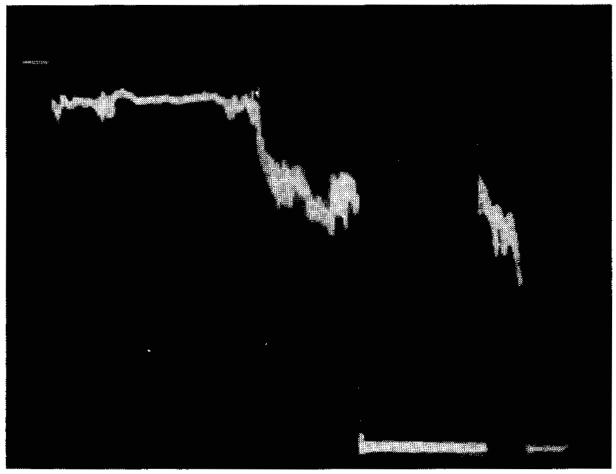

(a)

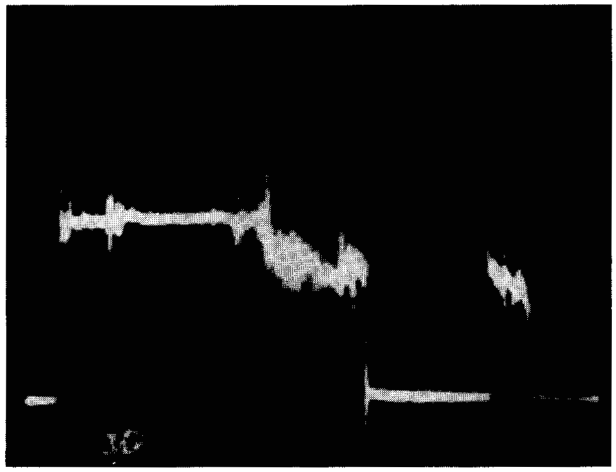

(b)

Figure 11

Writing waveforms for sample consisting of 13 nm Al_2O_3 on aluminum having 2 Ω/□ resistivity, with thin overlayer of graphite in binder; underlayer was smooth cross-linked CAB. Single-phase driver used with 200 Ω internal impedance at –70 V output. (a) Voltage across sample; 10 V per vertical division, 10 μs per horizontal division. (b) Current through sample; 50 mA per vertical division, 10 μs per horizontal division.

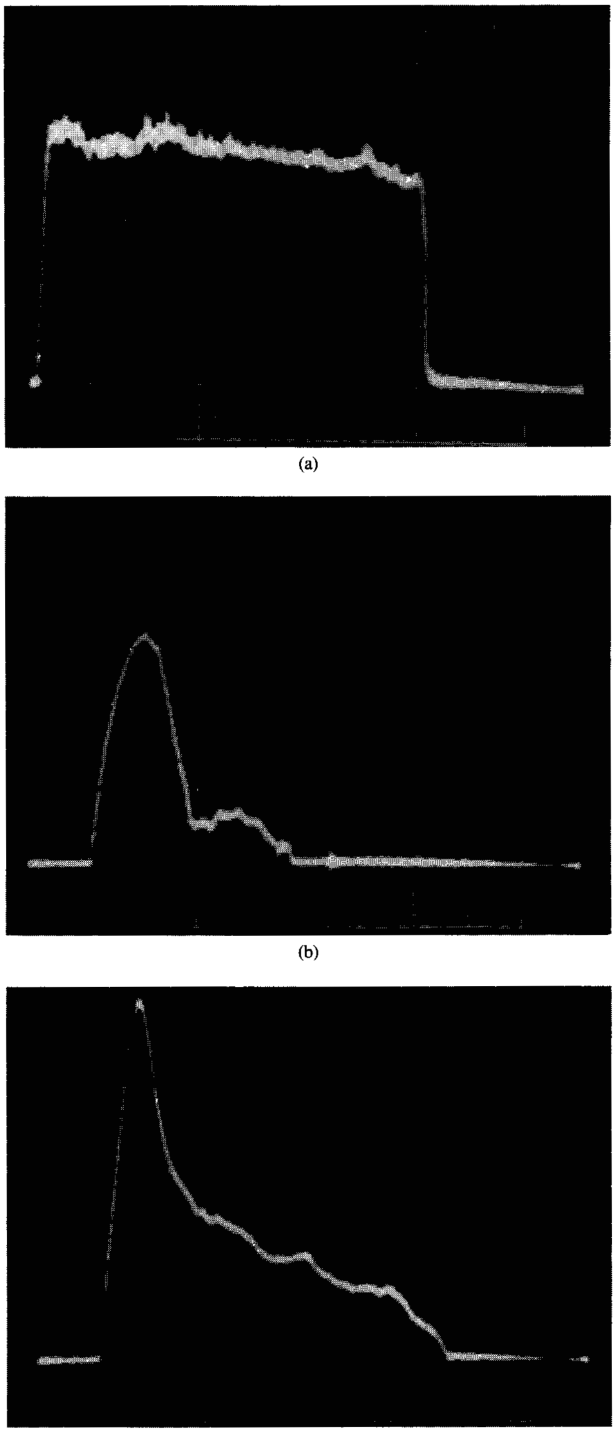

(a)

(b)

(c)

Figure 12

Writing waveforms for various applied voltages using low-impedance, single-phase driver. Sample consisted of 45 nm of aluminum with overlayer of graphite in binder; underlayer was smooth, cross-linked CAB. (a) –13 V applied; 50 mA per vertical division, 50 μs per horizontal division. (b) –25 V applied; 250 mA per vertical division, 1 μs per horizontal division. (c) –35 V applied. 250 mA per vertical division, 1 μs per horizontal division.

driving circuit to initiate the necessary arc between a stylus and the aluminum film (see the Appendix).

The drive circuit initially employed in the present studies was of high output impedance (about 200 Ω) and relatively high voltage (50 to 100 V). This circuit gave poor writing on smooth, hard samples simply because an electric arc was rarely initiated. Instead, a constant current flowed into the aluminum film through the large area of the stylus–aluminum contact; such a large contact area is characteristic of writing on smooth surfaces. As shown by the waveforms of **Figure 10**, the equivalent resistance of this contact was about 40 Ω. Because of the high internal impedance of the driver, this current was insufficient to raise the local temperature by Joule heating high enough to remove the aluminum. Since direct electrical contact was never broken, a potential across the structure sufficiently large to sustain an arc was not generated. On the other hand, the circuit gave good writing for those kinds of samples permitting only limited contact area, since in that case the current density was high enough for pronounced localized heating. The electric contact was consequently broken by disintegration or melting of the aluminum caused by Joule heating, so that the arc could subsequently start. Such samples either had a rough substrate surface, so that good contact was achieved only on the peaks, or alternatively had a smooth but soft substrate, so that the distortion of the substrate under the stylus permitted contact only over small areas, e.g., samples made from the metallized polyester sheet discussed in Part II.

- *Successful writing with high-impedance driver*

In spite of the difficulties just discussed, a technique was found which did permit improved writing of smooth, hard-substrate samples with the high-impedance driver.[9] For this purpose, a thin insulating layer was deposited over the aluminum film so that no direct stylus–aluminum contact was permitted. When a voltage pulse was applied to a stylus, an arc was initiated by local dielectric breakdown through the insulator. For a 70-V pulse, the voltage and current waveforms are shown for such a sample having an insulating film of aluminum oxide 12.5 nm thick (**Figure 11**). The varying waveforms are associated with arcing; it is noted in fact that the arcing self-limits after about 60 μs, but is followed by a short arc burst after a pause. Inspection of the sample after such writing shows large hole sizes, in contrast to samples without the insulating overlayer.

Various materials have been used successfully as the insulating layer, including polymer films as well as metal oxides. Such films must exhibit dielectric breakdown at relatively low voltages while being easily disintegrated by the arc.

[9] See footnote 2.

Successful writing with low-impedance driver

The insulating overlayer is not required for writing if the internal impedance of the driver is lowered sufficiently. Under these circumstances it should be possible to deliver enough current to cause extensive metal removal even for the large stylus–metal contact area given by hard, smooth samples. A low-impedance (less than 1 Ω), high-current driver was used to provide pulses at various voltages, resulting in the current waveforms shown in **Figure 12**. For a 13-V pulse a constant current was delivered for the full length of the pulse. The power delivered was apparently insufficient to cause any change in the sample by Joule heating. In contrast, a 25-V pulse caused a 1-A peak current, while a 35-V pulse caused a peak current as high as 1.8 A; holes in the aluminum were observed in both cases, with larger holes for the 35-V pulse. Because these holes were generated by Joule heating rather than arcing, they were more rounded in shape, with more uniform edges.

The current pulse extinguished itself when the hole was roughly the size of the stylus diameter. As the voltage increased above 35 V, the current pulse length markedly decreased, whereas the peak current increased nonlinearly with increasing voltage, as seen in **Figure 13**.

The major problem with the use of the low-impedance driver is that the current waveform, and hence the resulting written area, is highly dependent on the resistance presented to the driver. This was demonstrated by experiments in which the value of an added series external resistor was incrementally increased, thereby resulting in corresponding increases in the high-current pulse length simply because the resistor caused less power to be dissipated in the aluminum film. Since the current path passes through the aluminum film to ground, it was anticipated from these results that the sheet resistivity (related to thickness[10]) of the film influences the waveform; this conclusion was confirmed (**Figure 14**). Thus, even though more metal must be removed as the aluminum thickness is increased, the resulting lower sheet resistivity and consequent higher current gave a shorter net burn-out time for the thickness range of Figure 14. The contact resistance directly under the stylus is also important, as shown in **Figure 15**, where it is seen that the current waveform decreases in height and increases in length as the overlayer thickness is increased.

Although the written holes are more regular for the low-impedance driver case, the high-current requirement not only puts a high demand on the driver and power supply, but may cause crosstalk problems between styli. For these reasons the high-impedance driver with the insulated-overlayer structure (see the preceding subsection) may be a more attractive alternative for smooth samples.

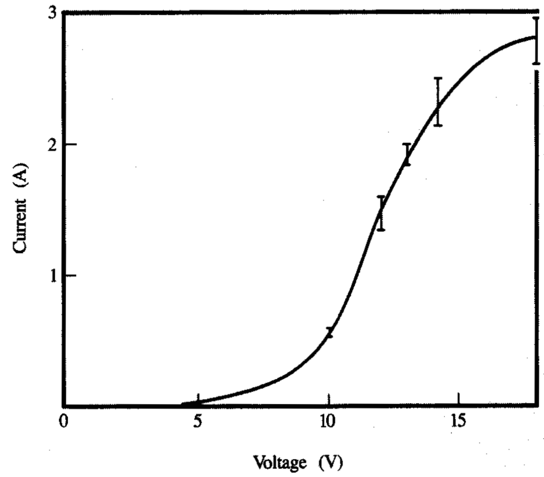

Figure 13

Peak write current as a function of writing voltage using a low-impedance, single-phase driver for a sample consisting of 44 nm of aluminum with a thin overlayer of graphite in binder; underlayer was smooth, cross-linked CAB. Several pulses were applied to determine each data point.

Disadvantages of smooth underlayer

Although two alternative means for writing smooth-underlayer samples were found, and although such samples exhibited very little scratching averaged over the written area, such material was judged to be impractical for the following reasons:

1. Even though little scratching was observed, very elongated scratches were produced in the few cases where scratching did occur. This result is in sharp contrast with scratching observed in rough-underlayer structures, which show a multiplicity of small, isolated scratched areas. This difference in characteristics is explained by the inability of scratches to propagate into the valleys of the rough-underlayer sample; there is little to stop a scratch on a smooth sample once it starts.
2. Smooth-substrate structures are particularly sensitive to surface inhomogeneities created either during fabrication or by the writing process. For structures incorporating an insulating overlayer for use with a high-voltage, high-impedance driver, insulating particles on the surface can prevent local dielectric breakdown

[10] Thickness measurements were carried out by taking profilometer traces of deposits made on glass substrates positioned in the vacuum chamber adjacent to the samples being metallized. Alternatively, the aluminum deposit was monitored by measuring the electrical sheet resistivity (expressed in Ω/□) with a four-point probe. This method was quick and reproducible, and permitted measurements directly on the sample. However, it should be noted that the relation between sheet resistivity and metal thickness is dependent on the roughness of the substrate: The rougher the substrate, the thicker the metal film required to achieve a given sheet resistivity.

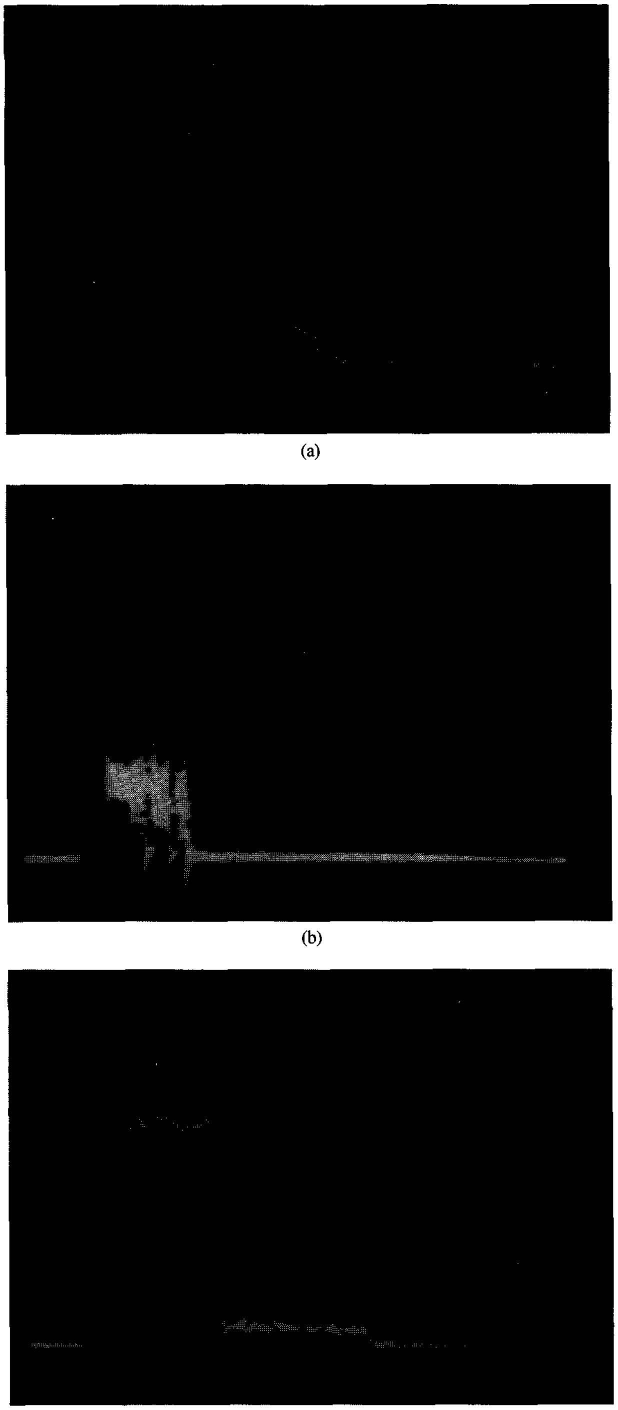

Figure 14

Effect on current waveforms of increasing the aluminum thickness using a low-impedance, single-phase driver for samples consisting of aluminum with a thin overlayer of graphite in binder; underlayer was smooth, cross-linked CAB. (a) 22 nm aluminum; 100 mA per vertical division, 5 μs per horizontal division. (b) 44 nm aluminum; 50 mA per vertical division, 5 μs per horizontal division. (c) 90 nm aluminum; 250 mA per vertical division, 2 μs per horizontal division.

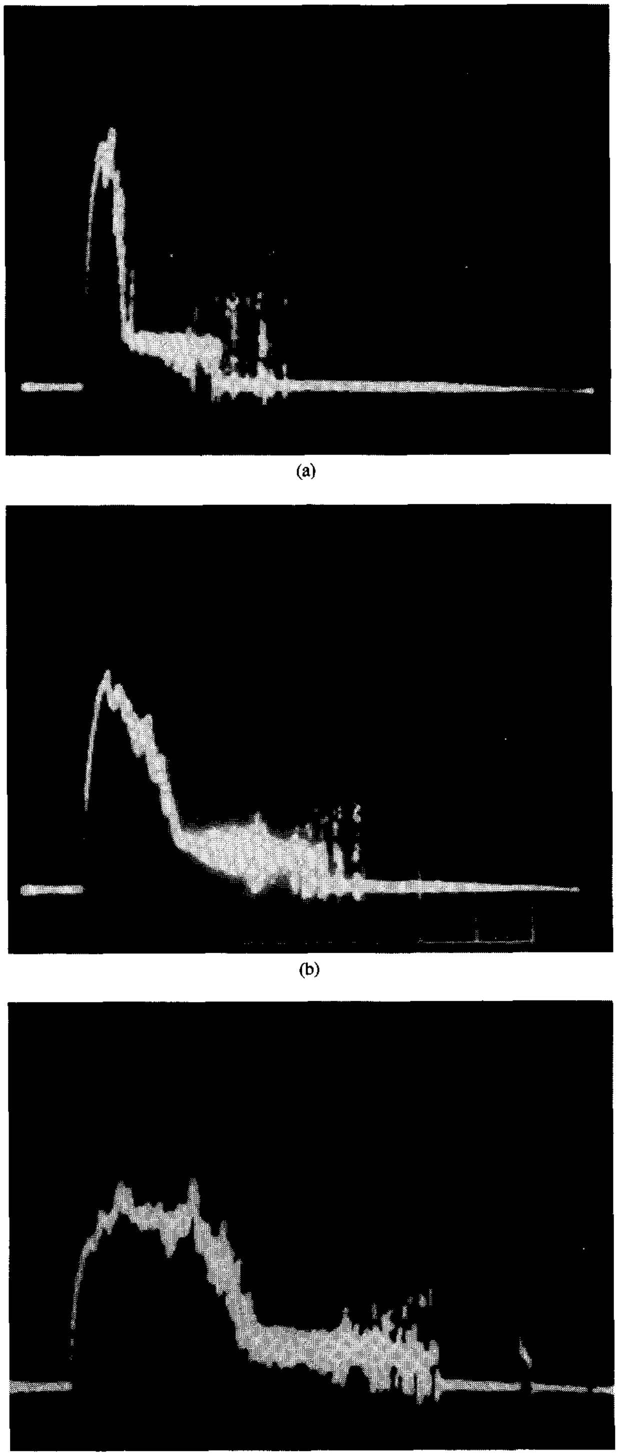

Figure 15

Effect on current waveforms of increasing the overlayer thickness using a low-impedance, single-phase driver for samples consisting of 44 nm of aluminum with an overlayer of graphite in binder; underlayer was smooth, cross-linked CAB. 100 mA per vertical division, 5 μs per horizontal division. (a) 9 $\mu g/cm^2$ overlayer. (b) 40 $\mu g/cm^2$ overlayer. (c) 74 $\mu g/cm^2$ overlayer.

and hence inhibit uniform writing. Similarly, for structures without the insulating overlayer for use with a low-voltage, low-impedance driver, extraneous surface material has been found to increase the circuit resistance and change the current waveform in the manner described above. These mechanisms can contribute to local variability in writing quality.

3. In contrast with rough-underlayer structures, no scouring action is available to remove debris generated during writing. Such accumulated debris on the styli can foul the electrodes so as to suppress writing (see Section 5).

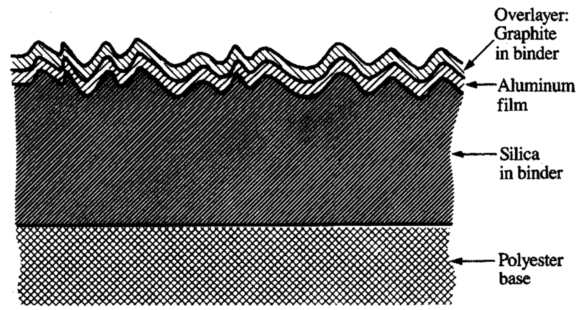

Figure 16

Schematic representation of the structure of a rough-underlayer sample. (Not to scale.)

4. Rough-underlayer samples

As pointed out above, the rough-underlayer structure proved to be more advantageous than the smooth, and was therefore investigated in greater detail. The study of smooth-underlayer samples was beneficial, however, since it added to the understanding of the behavior of and requirements for the preferred rough-underlayer samples.

- *Structure of rough-underlayer samples*

The structure of a rough-substrate sample is illustrated in **Figure 16**. The substrate was 50 to 75 μm thick, and consisted of polyester which was often specially treated to improve adhesion of subsequent coatings. The underlayer was about 5 to 10 μm thick and was composed of silica particles with diameters of a few μm in a cross-linked cellulosic binder (CAB). The aluminum layer was 20 to 30 nm thick and was fabricated by vacuum deposition. The overlayer had an average areal density in the range of 1 to 10 $\mu g/cm^2$ and consisted of graphite in an organic binder. It, as well as the underlayer, was applied by organic-film coating techniques. It should be noted that the concentration of silica particles in the binder, i.e., the pigment volume concentration (PVC),[11] is a major determinant of the roughness of the underlayer. (Details of improved fabrication techniques for rough-underlayer DNP material may be found in Part II.)

It is important to control the particle size and dispersion of the silica in the underlayer so that the surface roughness is properly determined. A typical profilometer trace of an early sample is shown in **Figure 17**.

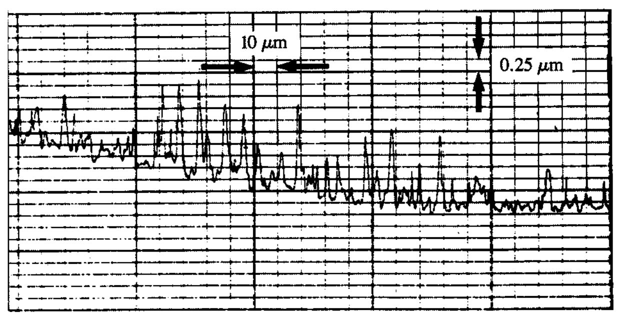

Figure 17

Profilometer trace of a rough-underlayer sample. Underlayer consisted of 10% PVC silica in cross-linked CAB.

- *Driver electronics*

As discussed in Section 3, arc initiation is difficult with *smooth* samples when using a high-impedance, low-current driver because of the low resistivity of the intimate stylus–aluminum contact. In contrast, the Joule heating provided by a low-impedance, high-current driver can erode away the aluminum associated with this contact, but subsequent arc maintenance is impeded by the low voltage of such a driver.

Intimate contact is also achieved between the stylus and the aluminum for *rough* samples, but now only at the localized regions associated with the peaks of the rough surface. Before an arc can be initiated, these contacts must be opened by aluminum removal caused by Joule heating, which can in fact be accomplished in the rough-underlayer case by a high-impedance driver. However, the electroerosion process proceeds much more efficiently if a special two-phase driver is used.[12] During phase 1 a high-current, low-impedance circuit is used for the Joule-heating

[11] The pigment volume concentration of a coating formulation is defined as the volume of pigment divided by the total volume of pigment plus binder, where the volume of each component is defined by the ratio of its weight in the formation to its density.

[12] Circuit designed by G. Goldrian of the IBM Information Products Division, Böblingen, Germany.

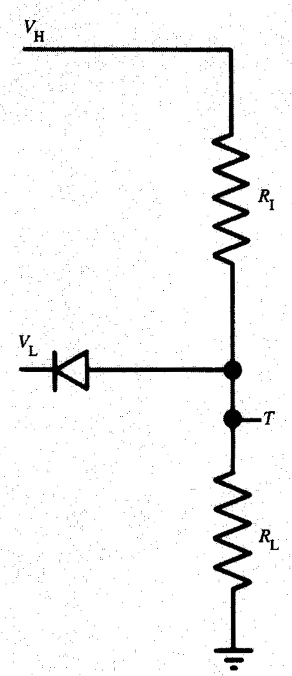

Figure 18

Schematic diagram of two-phase driver.

"initiation" process, i.e., opening of all direct contacts, while during phase 2 a high-voltage, high-impedance circuit is used for sustaining the arc. The transition from the first phase to the second is carried out automatically by the circuit of **Figure 18**. Here V_H and V_L represent high and low *negative* voltage sources, respectively, R_I is a resistor in series with the V_H source, and R_L is the stylus–aluminum contact resistance. The contact resistance R_L is initially low, so that upon triggering the circuit the voltage of the stylus tip (Point T) is clamped at V_L by the low-voltage supply. However, as phase 1 proceeds, aluminum is removed by Joule heating, and R_L consequently increases rapidly. When R_L becomes large enough that $V_H[R_L/(R_I + R_L)]$ becomes greater in magnitude than V_L, all of the current through R_L originates in source V_H, and source V_L is effectively excluded from participation because the diode is now reverse-biased. Unless otherwise noted, this two-phase driver circuit was used in the study of rough-underlayer samples. The parameter values were usually chosen to give $V_H = -48$ V, $V_L = -18$ V, $R_I = 200\ \Omega$.

- *Write test apparatus*

The two-phase circuit described above was used to drive the modified writing system (Section 1). In addition, the scratch tester (Section 2) was modified to permit the application of voltage pulses to its stylus. The resulting "write tester" permitted writing with a single stylus under a known mechanical force. An additional, special two-phase driver with a wide range of voltages and pulse lengths was built for use with this write tester.

Typical voltage and current waveforms obtained with the write tester are shown in **Figure 19**. A very high initial current pulse was associated with phase 1, which lasted for about 1 μs for the particular sample chosen. Following the automatic termination of phase 1, the voltage across the

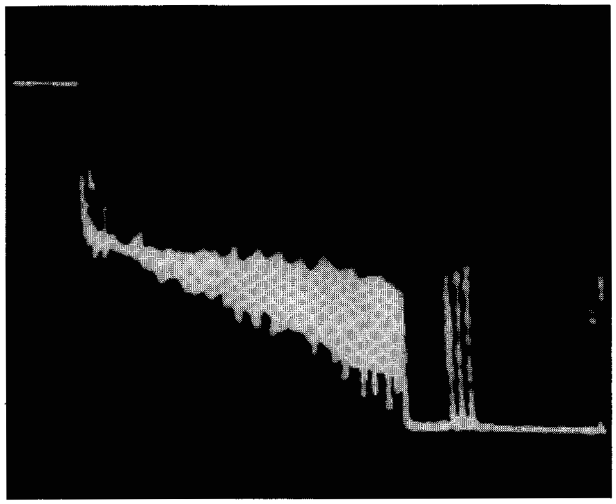

(a)

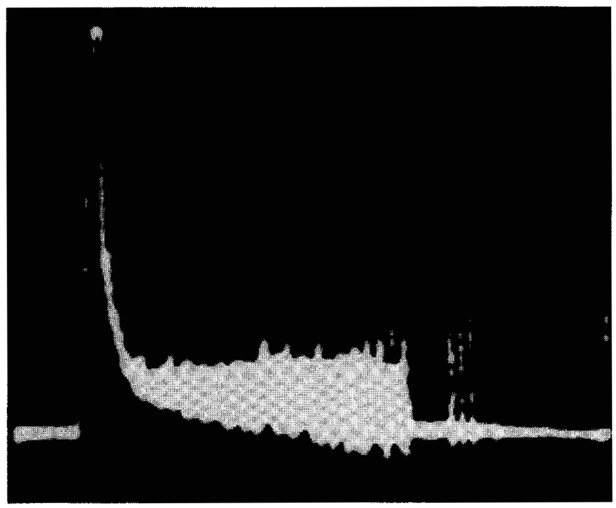

(b)

Figure 19

Writing waveforms for the two-phase driver; $V_L = -15$ V, $V_H = -30$ V. Sample had 14% PVC silica in CAB base layer with 1.7 $\Omega/\square$ aluminum film with 20 $\mu g/cm^2$ graphite-in-binder overlayer. (a) Voltage waveform; 5 V per vertical division, 5 μs per horizontal division. (b) Current waveform; 100 mA per vertical division, 5 μs per horizontal division.

sample increased and the current decreased as phase 2 began. The phase 2 current exhibited random spikes, as expected in a discharge phenomenon; short current "after-pulses" can be seen following termination of the main phase 2 pulse.

It is seen that the magnitude of the voltage across the sample increased during phase 2, while the average current was approximately constant or suffered a slight decrease. The impedance presented to the circuit by the sample thus increased during phase 2, corresponding to the increase in electroerosion of the aluminum under the stylus. Near the end of phase 1 about 20 V appeared across the sample, with an average current of approximately 150 mA. Such values are typical for a wide variety of samples.

- *Results of writing studies*

Testing was carried out on a wide variety of samples under different test conditions. Appreciable statistical variations in current and voltage waveforms were observed from place to place on the same sample, even though debris was carefully cleaned from the stylus before each test to improve reproducibility. Nevertheless, important relationships were clearly identified.

Phase 1

For rough-underlayer samples, stylus–aluminum contact occurs only in the regions near the peaks. Since phase 1 is associated with the removal by Joule heating of aluminum in direct contact with the stylus, it is clear that the phase 1 pulse becomes more pronounced if measures are taken to increase the net stylus–aluminum contact area. Thus, if the concentration of silica in the underlayer is decreased, the surface roughness decreases and phase 1 is more pronounced. Another way to increase the contact area is to increase the stylus force when writing a sample (see the Appendix). As seen in **Figure 20,** an increase of stylus force from 10 to 50 mN caused a pronounced increase in both the peak current and the pulse width. Alternatively, phase 1 becomes more pronounced if the stylus force is kept constant but the conductivity of the sample is increased, either by increasing the aluminum thickness or increasing the conductivity of the overlayer.

It is usually desirable to minimize the phase 1 pulse to reduce the demand on the electronic drivers in order to decrease the required total width of the writing pulse, and to decrease the total current flowing which could lead to interstylus crosstalk and unwanted electroerosion at the ground contact.

Phase 2

In rough-underlayer samples the bulk of the aluminum removal occurs in phase 2 rather than phase 1. Therefore, if the phase 2 current is artificially terminated, the resulting hole is smaller than if the pulse is allowed to proceed to

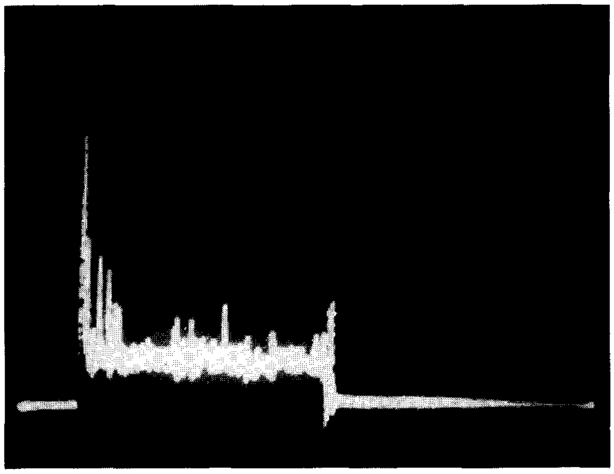

(a)

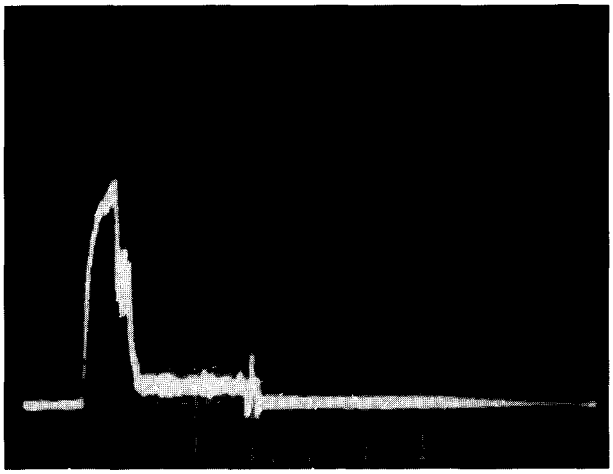

(b)

Figure 20

Effect of stylus force on current waveform. Sample had 14% PVC silica in CAB base layer with 90-nm aluminum film with 9 μg/cm^2 graphite in binder overlayer. (a) 10 mN stylus force; 100 mA per vertical division, 5 μs per horizontal division. (b) 50 mN stylus force; 250 mA per vertical division, 5 μs per horizontal division.

self-extinction, which occurs when the hole becomes somewhat larger than the stylus (**Figure 21**). It should be noted that the holes shown in Figure 21 are irregularly shaped and that some residue of unremoved material is left inside them.

The phase 2 current increases as the magnitude of the applied voltage V_H increases from 30 to 48 to 70 V (Figure 19 and **Figure 22**). Although the current increased by a factor of 5 in this series, the voltage drop V_T across the sample remained roughly around 20 V; in other words, the effect of increasing the applied voltage is effectively to decrease the impedance of the arc. (This property of voltage-drop constancy is characteristic of discharge

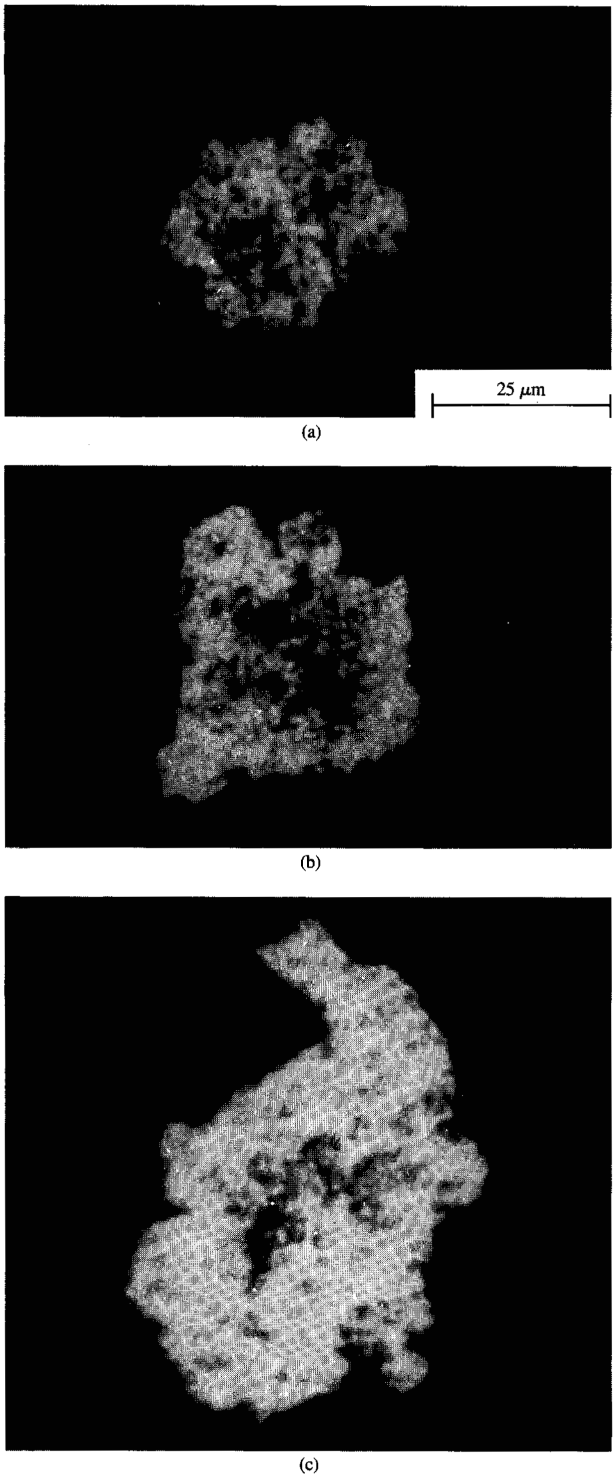

Figure 21

Transmission micrographs of eroded areas subjected to pulses of various lengths. Sample consisted of 1.4 Ω/□ aluminum with 30 μg/cm² graphite-in-binder overlayer; underlayer was 14% PVC silica in cross-linked CAB. Driver used –20 V during phase 1, –48 V during phase 2. (a) 2-μs pulse. (b) 4-μs pulse. (c) 8-μs pulse.

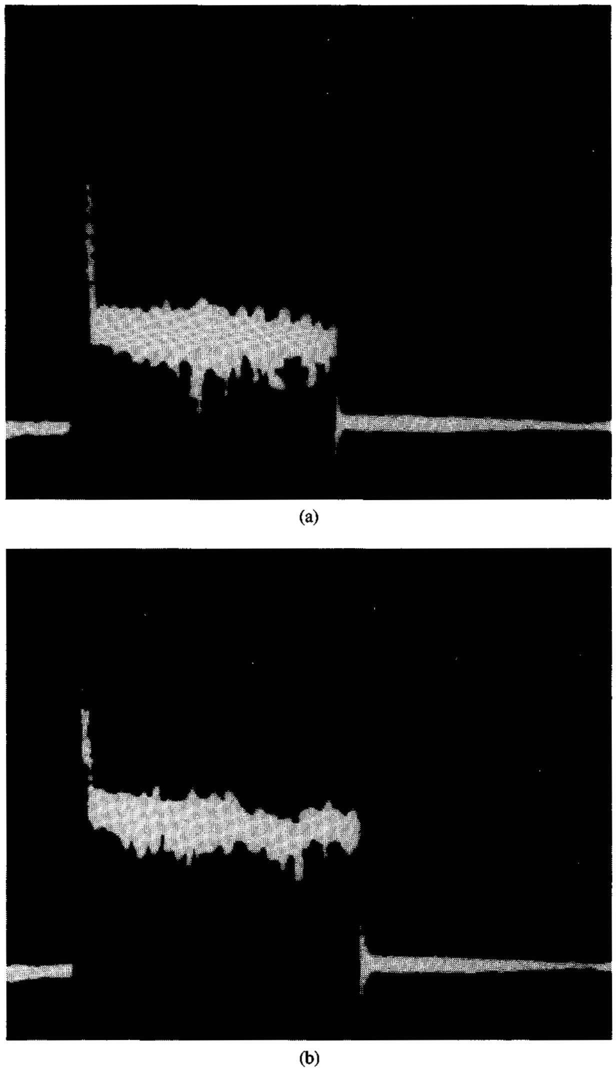

Figure 22

Increase in phase 2 current as the phase 2 voltage increases. Phase 1 voltage kept at –15 V. Sample consisted of 1.0 Ω/□ aluminum with 20 μg/cm² graphite-in-binder overlayer; underlayer was 14% PVC silica in cross-linked CAB. 100 mA per vertical division, 5 μs per horizontal division. (Also compare with Figure 19.) (a) –48 V. (b) –70 V.

phenomena; see the Appendix.) As expected, if the applied voltage was maintained constant and the value of the circuit resistor R_I was decreased, the current increased correspondingly. Thus, if $V_H = -48$ V, the current increased from 150 to 300 mA as R_I was decreased from 200 to 100 Ω.

Changing the stylus area by roughly a factor of 2 had no effect on the current. Because of the larger area involved, both phase 1 and phase 2 times were roughly doubled for the case of the larger stylus, but the eroded area was also doubled; i.e., the area eroded per unit time remained approximately constant.

Studies of eroded areas

To obtain a quantitative measure of the eroded area, a television camera was used in conjunction with a transmission electron microscope, with the output of the camera feeding a computerized image analyzer. When properly adjusted, this system gave a fast and convenient measurement of the eroded area even when that area was highly irregular in shape. Since there was a large statistical variation in hole size, three to six separate eroded areas were averaged for each writing condition. For each writing condition studied, the applied pulse length was varied and plots were made of the eroded area as a function of pulse length; such a curve will be called a *writing efficiency curve* (**Figure 23**). The increase in written (eroded) area for higher values of V_H is most pronounced for the longer pulse lengths. The saturation value of the eroded area, i.e., the area for a self-limiting pulse length, also increases for increasing values of V_H, since at higher values of V_H the arc extends further from the periphery of the stylus. The curves are closer together for short pulse lengths where phase 1 is an appreciable fraction of the total pulse length.

Changes in the structure of the sample can also affect these curves. Studies of eroded areas show that the slope of the writing efficiency curve is higher for samples with thinner aluminum, while **Figure 24** demonstrates that increasing the overlayer thickness causes a pronounced decrease in eroded area, presumably since additional energy is needed to remove the overlayer (see the Appendix).

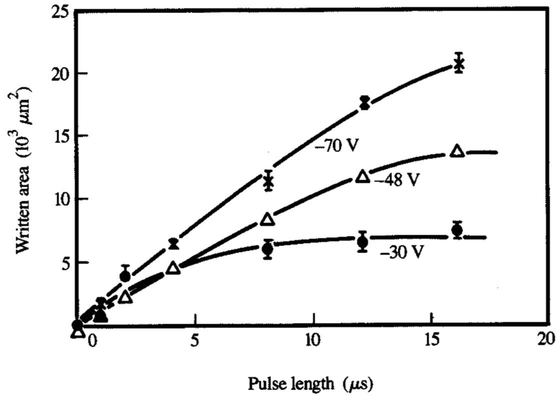

Figure 23

Writing efficiency curves: Written area (eroded area) vs. write pulse length for various values of phase 2 voltage. Phase 1 voltage was −15 V. Sample consisted of 1.0 Ω/□ aluminum with 10 μg/cm² graphite-in-binder overlayer; underlayer was 14% PVC silica in cross-linked CAB.

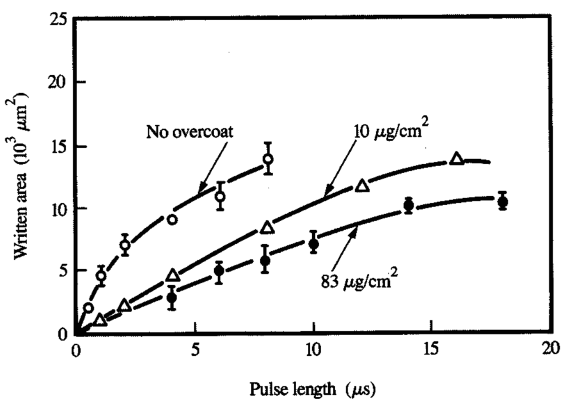

Figure 24

Writing efficiency curves: Eroded area vs. write pulse length for various graphite-in-binder overlayer thicknesses. Phase 1 voltage was −15 V; phase 2 voltage was −48 V. Sample consisted of 1.0 Ω/□ aluminum with graphite-in-binder overlayer; underlayer was 14% PVC silica in cross-linked CAB.

- *Writing vs. scratching*

As previously emphasized, a major goal of the present work is the suppression of scratching while maintaining adequate writing quality. To study the relationship between scratching and writing further, several series of 5 × 5-cm samples were written with the modified electroerosion system under identical conditions. The optical transmission was then measured with a microscope with the aid of a photodiode-based system.

The written (write power on) and the scratched (write power off) areas were measured separately; in each case the area of interest was positioned so as to fill the field accepted by the photodiode. For the scratched area, the optical transmission of the virgin background was subtracted from the transmission of the scratched area; ideally the transmission of the scratched area should be negligible.

The results of a study of scratching and writing as a function of overlayer thickness are illustrated in **Figure 25**. Here, after each write-scratch operation a thin increment of graphite-in-binder overlayer was applied to a sample. The thickness of the overlayer is given in terms of its areal density. (The overlayer was so thin that it was operationally more practical to characterize it by its optical density initially, and then later relate the optical density to the areal density by weighing thick-overlayer samples.) It is seen from Figure 25 that the optical transmission for writing decreases monotonically with increasing overlayer thickness, in accord with the results displayed in Figure

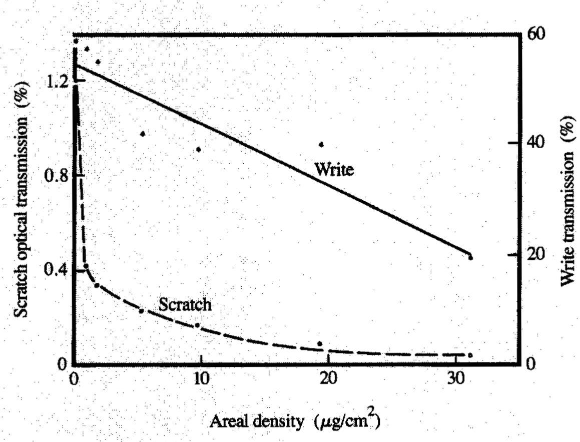

Figure 25

Optical transmission vs. areal density of graphite-in-binder overlayer for both written and scratched areas. The sample had an underlayer of 10% PVC silica in a cross-linked CAB binder, with an aluminum layer of 2.7 $\Omega/\square$ resistivity.

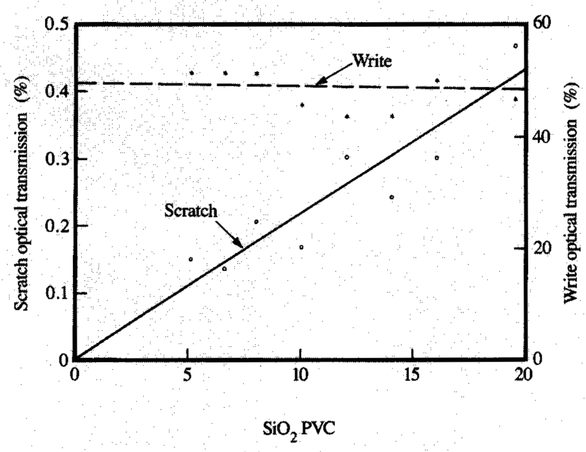

Figure 26

Optical transmission vs. silica PVC for both written and scratched areas. The samples had underlayers of various PVC values of silica in a cross-linked CAB binder, with an aluminum layer of 2.7 $\Omega/\square$ resistivity. A graphite-in-binder overlayer of about 4.4 μg/cm^2 was used in all cases.

24. The optical transmission for scratching similarly decreases with increasing overlayer thickness. However, it is noted that pronounced scratch suppression is given even by an extremely thin overlayer, while relatively small additional scratch protection is given by further increases in overlayer thickness. These results indicate that considerable scratch protection can be achieved with an overlayer having an areal density as low as a few μg/cm^2 without affecting writing quality. This is a fortunate result, since relatively little head fouling occurs for small overlayer thicknesses (see Section 5).

The same measurement techniques were used to examine a series of samples made with various values of surface roughness (PVC of silica in the underlayer), but with fixed aluminum and overlayer thicknesses (**Figure 26**). Here it is seen that the scratch optical transmission increases linearly with increasing PVC (the curve was forced through the origin), as anticipated from earlier results (Section 2). In contrast, the writing efficiency shows little dependence on surface roughness in this range.

- *Alternative materials*

Alternative materials have been used for the rough-underlayer structure. The rough underlayer has been fabricated by the incorporation of pigments other than silica, such as iron oxide or titanium oxide.[13] Also, other metals such as tin or magnesium have been used in place of the aluminum layer. While such samples may differ in details of their behavior, waveforms and electroerosion patterns similar to those discussed above were observed.

The choice of overlayer material is more critical. The graphite imparts lubricity and electrical conductivity to the overlayer, while helping to suppress electrode fouling. If an alternative insulating overlayer is used, e.g., if the graphite is omitted entirely, writing can still be observed, but only if the overlayer is thin enough to permit dielectric breakdown. If such overlayers are too thick, the dielectric breakdown becomes erratic, resulting in irregular phase 2 waveforms and small, irregularly shaped holes.

5. Head fouling

The high-temperature electrical discharge associated with the electroerosion process creates debris which can cause unacceptable degradation in writing quality. This debris includes not only aluminum, but also material which is primarily organic in nature. Such material is deposited on the styli and in the interstices between the styli, as well as being scattered over the surface of the sheet being written. The buildup of debris on a stylus is illustrated in **Figure 27**, which shows the end of a stylus before and after writing a track only a few cm long on a rough-substrate sample.

At times debris buildup has been shown to cause significant widening of the phase 1 pulse with repeated write operations for smooth-underlayer samples, indicating an increase in the contact conductivity associated with the

[13] Silica has a refractive index closely matching that of the CAB binder. Underlayers incorporating silica therefore offer less haze in transmitted light than do samples fabricated with these other pigments.

debris. On other occasions, total cessation of writing has been observed for both smooth- and rough-based samples when the debris has been insulating in nature. The effect upon writing efficiency thus depends upon the electrical conductivity and thickness of the accumulated debris layer.

Not only the overlayer but also the underlayer can contribute to fouling, as shown by the fact that electroerosion *paper*, which has no overlayer, also exhibits fouling under certain circumstances. No matter which layer contributes most to fouling, it seems probable that the higher the degradation temperature of the material, the less the fouling. To test this concept, some samples were

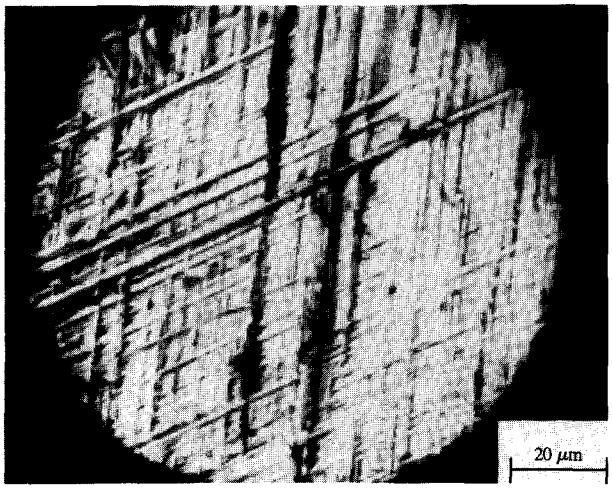

(a)

(b)

Figure 27

Micrographs of the tip of a stylus (a) just after polishing on abrasive paper; (b) after writing a track a few cm long in a sample consisting of 1.4 Ω/□ aluminum with 30 $\mu g/cm^2$ graphite-in-binder overlayer; underlayer was 14% PVC silica in cross-linked CAB.

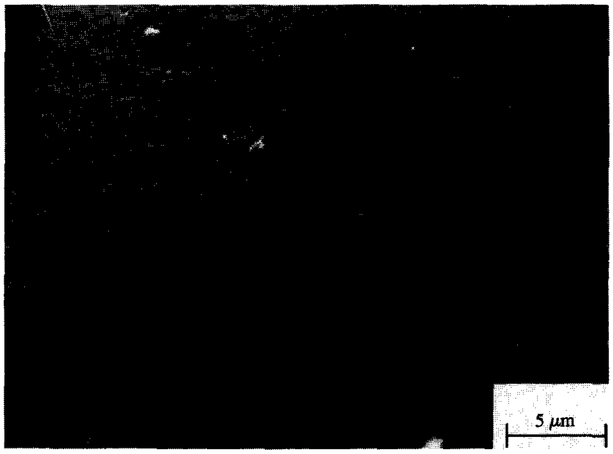

(a)

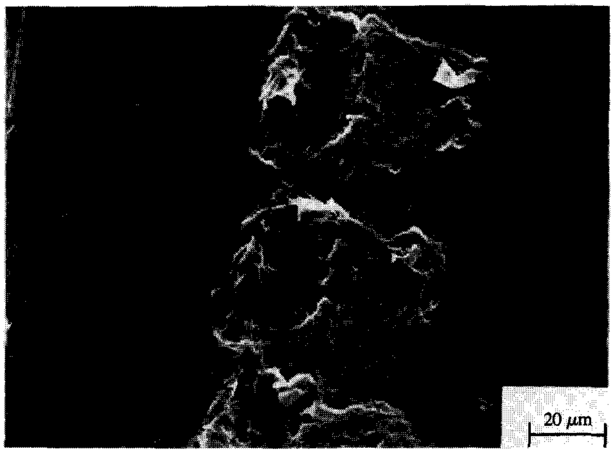

(b)

Figure 28

Contribution of organic components of the sample to fouling. Scanning electron micrographs of smooth samples after writing and after removal of the overlayer and aluminum. (a) Highly cross-linked silicone substrate. (b) Polyester substrate.

prepared in which the substrate consisted of a hard, highly polymerized silicone resin known to withstand higher temperatures than hydrocarbons; for comparison, samples consisting simply of aluminized polyester were also examined. After both sets of samples were written, the overlayer and aluminum layer were dissolved off. In both cases pits could be seen in the written areas under the microscope, but these pits were much less pronounced in the silicone-underlayer case (**Figure 28**). From practical considerations of manufacturability and cost, hydrocarbon materials may nevertheless be more suitable for incorporation into the overlayer and underlayer. In this case, the decomposition product ideally should be a nontoxic gas or a particulate residue with light, free-flowing characteristics so that it does not adhere strongly to the writing head or otherwise affect operations of the electroerosion printer. Various candidates for binders were tested by heating in air at about 250°C. In this way it was found that several simple cellulosic materials, e.g., CAB, did in fact reduce to a light, powdery, charcoal-like consistency, while some other materials such as polyethylene oxide or polyvinyl alcohol were either hard or gummy.

One of the purposes of the rough underlayer is the scouring of debris from the bottom of the styli. Sufficient roughness must be attained to permit debris removal by abrading at a rate which is at least as fast as the buildup caused by writing. This scouring action cannot, of course, take place for smooth samples, for which very severe fouling is often observed. For smooth samples it was found that after only one write pulse the stylus was nearly completely covered with debris; fouling in such samples was often severe enough to cause poor writing quality after a writing path of only a few tens of centimeters. However, samples with underlayers containing a silica PVC of more than about 5 percent appeared to give a scouring action which was adequate to inhibit fouling if the underlayer and overlayer were properly formulated.

While the details of the fouling process are poorly understood, these studies nevertheless showed that fouling did not cause a short-term writing problem for a properly fabricated rough-underlayer sample containing a cellulosic underlayer and overlayer. In this case the debris was removed from the tips of the styli as fast as it accumulated. On the other hand, it was found that debris quickly accumulates in the head adjacent to the insulator block in the interstices between the protruding styli. This debris is initially a harmless powder, but with continued writing the deposit can slowly transform into a hard cake which can be removed only by vigorous mechanical scrubbing. The hard cake grows slowly until it extends to the tips of the styli, at which point the writing efficiency suffers a marked decrease. Because of its slow, cumulative nature, this long-term fouling problem required testing of large areas of DNP material; i.e., full rolls were required. This subject is discussed in Part II.

6. Conclusions

This paper offers a foundation for the design of the direct negative and the direct plate by showing that it is possible to solve the basic problem of mechanical scratching while preserving writing efficiency.

Acceptable results were obtained when a mechanically hard, rough layer was applied to the polyester substrate, while a very thin lubricating layer having some electrical conductivity was applied over the aluminum. These measures were effective because they permitted acceptable writing while eliminating substrate deformation and reducing adhesive wear.

The underlayer was composed of silica particles in an organic binder, while the overlayer consisted of graphite particles in a binder. Even though scratching is less in smooth- rather than rough-underlayer samples, rough rather than smooth underlayers were preferred because the writing operation was thereby made more reproducible. In particular, debris created during writing was scoured away from the styli in rough-underlayer samples, while the occasional elongated scratches seen in smooth-underlayer samples were not present with rough underlayers. Such rough-underlayer samples can be written successfully with a two-phase driver. The first phase of this driver provides a high current for Joule heating, which causes breaking of direct local aluminum–stylus contacts; the second phase provides an arc which removes the remainder of the aluminum under the stylus. However, since removal of the overlayer requires additional writing energy, in order to utilize short write pulses care must be taken to use the minimum overlayer thickness consistent with acceptable scratching.

Probably the least understood problem encountered is that of head fouling. Organic debris generated during writing collects around the styli, but it appears that this debris is continually abraded away by the mechanical action of the rough substrate, thus preventing degradation of writing quality by fouling in the short term.

Appendix: Physics of writing

For brevity some aspects of the physics of writing rough-underlayer samples were omitted from the body of the text and are discussed here. An attempt is made to relate these studies to literature of other fields.

- *Phase 1—Joule heating*

As pointed out in Section 4, the initial portion of the write pulse is associated with local removal of the metal layer by melting or disintegration caused by Joule heating. This is important because only after the opening of the stylus–aluminum contact can the arc phase begin. The electrical resistivity which governs Joule heating depends on the effective contact area between the stylus and the aluminum layer. The contact area depends in turn upon the force on the stylus, the morphology of the surfaces involved, and the mechanical properties of the materials.

Local regions of high mechanical pressure can be expected because the sample substrate is deliberately made rough, while the stylus face is always microscopically rough. Hertz showed that in the regime of perfect elasticity, a rigid ball pressed against a planar surface ideally generates a circular contact of area A given by

$$A = 2.43(Wr/E)^{2/3}, \tag{A1}$$

where W is the applied force, r is the radius of the ball,

E is the modulus of elasticity of the sample, and 0.3 is assumed for the Poisson ratio.

As the force W is increased [20], the contact area increases until the elastic limit of the material is reached, which occurs first at the region of high pressure near the periphery of the contact area. As the force is increased still further, an increasingly larger portion of the contact area is in the plastic-flow rather than the elastic regime. When the force is large enough that the behavior is described entirely by plastic flow, the contact area is given by

$$A = W/P, \tag{A2}$$

where P is a measure of the hardness of the sample (the average pressure on a spherically tipped indenter).

Because of the morphology of the surface, the stylus is supported on not one but several peaks of various heights; the higher peaks are in the plastic-flow regime, while some of the lower peaks are in the elastic regime. In this case Equation (A2) does not strictly hold, but can be made valid by the insertion of a constant of proportionality [21].

Stylus–aluminum electrical contact, therefore, is made only at these peaks; i.e., the current is constricted to flow through small areas. When two large-area conductors make contact only in small regions of total area A, the current through the conductors is governed [21] by the associated "constriction resistance"

$$R_c = (\rho_1 + \rho_2)(\pi/16A)^{1/2}, \tag{A3}$$

where ρ_1 and ρ_2 are the resistivities of the respective conductors. From Equations (A1)–(A3), the constriction resistance is then proportional to $W^{-1/3}$ in the elastic regime and to $W^{-1/2}$ in the plastic-flow regime; the important point is that in either regime the resistance decreases with increasing stylus force (compare Figure 20).

When current is passed through the contact regions, the metal can become hot enough to melt and to vaporize; this effect has been studied for solid metal contacts [21, 22]. Since conductive flow of electric current follows laws similar to those for heat energy, a relation between temperature and electric potential can be derived. Upon integration, this relationship becomes

$$\theta_m^2 - \theta_0^2 = V_c^2/4L, \tag{A4}$$

where θ_m is the maximum temperature in the conductor, θ_0 is the temperature in the conductor far from the junction (room temperature), V_c is the voltage drop across the contact, and L is the Lorentz constant [2.45×10^{-8} (V/K)^2] in the Wiedemann–Franz law. Thus, if a current through the contact generates a voltage drop of V_c, the maximum temperature θ_m induced in the contact by Joule heating is given by Equation (A4). Therefore, corresponding to melting and boiling temperatures for each metal there are melting and boiling *voltages*, which for most metals are about 0.5 and 1 V respectively; i.e., if the voltage across the junction achieves these values, the metal begins melting or boiling.

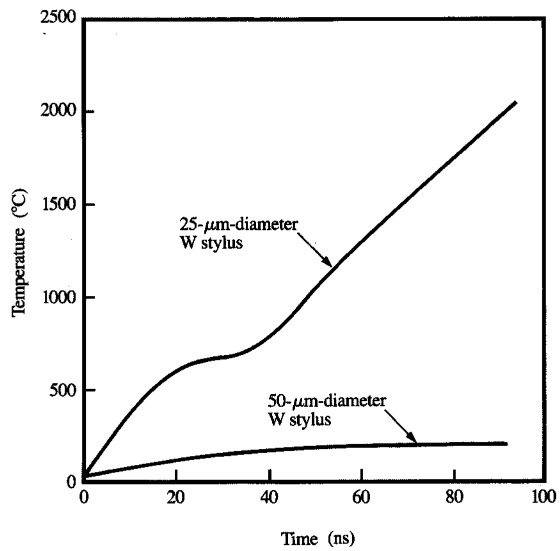

Figure 29

Computer simulation of temperature vs. time during writing operation. Assumed 5 W absorbed in aluminum during writing pulse.

These considerations help explain results of writing experiments described in Sections 3 and 4. A large total stylus–aluminum contact area may be achieved either by writing on a relatively smooth sample (e.g., low value of PVC of silica) or by applying very high stylus force for a sample of given roughness. In either case, the contact resistance will be low enough that a high current can be passed through the contact points without exceeding either the melting or boiling voltages. For the two-phase driver a large phase 1 current pulse can then be expected. If a single-phase, high-impedance driver is used, the voltage developed across the contact may never be large enough to achieve the melting or boiling voltages necessary to open the contact (compare Figure 10).

In order to obtain another perspective on temperatures attainable by Joule heating, a computer simulation was made of temperature vs. time in a 50-nm aluminum film on an insulating substrate. It was assumed that 5 W of power was absorbed in the aluminum in an area alternatively 25 or 50 μm in diameter, and that heat was lost both to the substrate and to the tungsten stylus. In the 25-μm case (**Figure 29**), the curve first rises, then levels off until the aluminum is totally melted, and then rises rapidly, all in tens of ns. However, if the power is spread over a

50-μm-diameter area, the curve saturates at a temperature well below melting. These results show that Joule heating can indeed destroy local direct stylus–aluminum contact in tens of ns (small phase 1), but only if the contact area is initially small enough to constrict the heat flow.

- *Phase 2—Arc*

An arc is initiated after direct electrical contact is broken by Joule heating. At least for the preferred rough-surface samples, it is the arc which in fact does the real work of metal removal. Some insights into the physics of the electroerosion arc may be gained by a study of the literature relating to switching arcs. When the electrodes of a switch are in close proximity (of the order of 1 μm) on either the "make" or "break" cycle, an arc can occur between the electrodes; temperatures high enough to cause metal removal from the electrodes are easily attained in the presence of such an arc. There has been much interest in the physics of such "short" arcs because of telephone-relay applications [23–29].

It has been pointed out [24] that these arcs are not associated with ionized air, but rather with the ionized vapor of the metal of the switch contacts. This concept is easily demonstrated by noting that, according to Paschen's law, the initiation voltage of an arc is a function of the product pd, where p is the gas pressure and d is the electrode spacing. The curve of initiation voltage vs. pd has a minimum, which for air is about 300 V. Air-supported arcs must therefore be excluded from consideration, since short switching arcs can easily be observed at 50-V electrode potentials in small gaps; such arcs are also seen when switches operate in vacuum.

The mechanisms proposed for initiating short switching arcs do not involve the usual Townsend multiplication process, but rather arc initiation by field emission from sharp projections on the cathode surface [25, 26]. High-current field emission is followed by vaporization of metal from either the cathode, because of the very high current densities in the vicinity of these projections, or the anode, because it is subjected to consequent local electron bombardment. In either case an arc is established in the resulting metal vapor, which is boiled off the electrodes [23–27]. A plasma of ionized metal atoms is thereby created between the electrodes, and metal is typically removed from both the cathode and the anode [27]. However, it has been found [27, 28] that metal removal from the anode predominates at small interelectrode distances and lower voltages, giving an "anode" arc, while metal removal from the cathode predominates at larger interelectrode distances and voltages greater than 300 or 400 V, giving a "cathode arc." The behavior of the arc in this regard has been found to depend quantitatively on the ionization potential and vapor pressure of the electrode metals [28]. A complicating factor in predicting the metal-removal rate is the influence of thin layers of carbonaceous material on the electrode surfaces; such layers are easily produced by repeated arcing in the presence of organic vapor and usually enhance arcing and metal erosion [25].

A study of the metal-removal mechanism in short switching arcs shows that this mechanism cannot be described merely as metal evaporation, but involves the ejection of molten droplets from the electrode [29]. An investigation of the use of DNP material as a direct plate (see Part III) has revealed similar behavior for the electroerosion of DNP material.

The conditions for the electroerosion arc are thus seen to be very similar to those for the short switching arc. The main difference is that in the electroerosion case the material for one of the electrodes is a very thin film which is not pitted, but instead locally totally removed by the action of the arc. The arc therefore does not reside in one area, but moves about as the metal from original areas is consumed. The details of the metal-removal mechanisms are not well understood in the electroerosion case, but besides metal evaporation these mechanisms may involve rapid disintegration of the metal film by concurrent ablation of a portion of the underlying polymeric material. The fact that a small portion of the organic substrate beneath the aluminum layer is also removed during the electroerosion process lends support to this view.

From the discussion on switching arcs it is also clear that anode arcs predominate for the voltages and spacings utilized in electroerosion. For this reason the electroerosion of aluminum is expected to be enhanced if the tungsten styli are made the negative rather than the positive electrodes, as is confirmed in practice.

It is possible to postulate that the electroerosion arc is initiated in the metal vapor generated by Joule heating during phase 1, rather than by the field-emission mechanism which is accepted for switching arcs. To test this postulate, both waveforms and resulting hole sizes were studied for a stationary single stylus for the case of a continuous pulse 14 μs long, and for the case of seven pulses each 2 μs long separated by waiting times of several seconds. Repeated trials showed identical results upon comparing the continuous- and interrupted-pulse cases, leading to the conclusion that the Joule heating of phase 1 does not in fact cause arc initiation directly. On the other hand, it is clear that arc initiation cannot take place until an adequate interelectrode potential drop is provided by the elimination during phase 1 of the direct stylus–aluminum shorts associated with the peaks of the rough surface.

- *Influence of the overlayer on writing*

It was pointed out in Section 4 that writing efficiency is decreased by the presence of an overlayer film. It is possible to postulate two different mechanisms for this effect:

1. Addition of the overlayer does not affect the arc itself, but makes the arc less effective in the aluminum-removal process because additional energy is now required to erode the extra overlayer material.
2. Because of the dielectric nature of the overlayer, the arc is electrically suppressed, so that more time is needed for successful writing.

The evidence points to the first mechanism. First, as noted in Section 4, the phase 2 current is not appreciably changed by the addition of the overlayer, as would be expected if the overlayer suppressed the arc; instead, it is found that the pulse length required for successful writing is merely increased. Second, special structures were fabricated to test the postulated arc-suppression mechanism. Here a structure of graphite-in-binder on aluminum (Structure A) was fabricated on the usual rough underlayer **[Figure 30(a)]** together with a sandwich structure (Structure B) of aluminum on graphite-in-binder on aluminum **[Figure 30(b)]**. The two structures were identical in every respect except for the additional aluminum overlayer of Structure B. Structure A had an overlayer thickness large enough to require about 16 μs for writing. If the arc-suppression mechanism is in fact decisive, the writing time for Structure B should be shorter than that for Structure A, i.e., about 4 μs, typical of no-overlayer samples at the standard voltages. The required writing time for Structure B was in fact as long as that for Structure A; i.e., the presence of the top aluminum layer did not improve the writing efficiency by improving the aluminum–stylus contact. These results prove that in standard thin-overlayer samples the graphite of the overlayer provides enough conductivity to ensure arcing, but the writing rate is limited by the rate of removal of the overlayer. On the other hand, if the overlayer is thick and insulating rather than thin with some conductivity provided by the graphite, inhibition of the arc can in fact take place (Section 4). In this case dielectric breakdown must be invoked as participating in the resulting discharge phenomena.

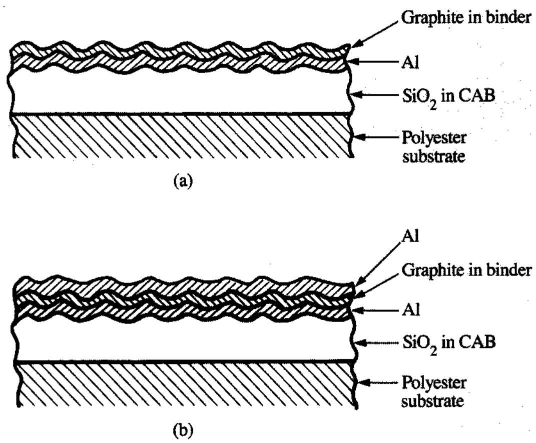

Figure 30

Structures for experiment for studying arc initiation process. (Not to scale.) (a) Structure A: Graphite-in-binder on aluminum. (b) Structure B: Aluminum on graphite-in-binder on aluminum.

Acknowledgments
The work of only a few of the many people who contributed to this study can be acknowledged here. A. Afzali, K. Sachdev, and J. C. Shen made significant original contributions to the chemistry involved in fabricating the various structures. C. R. Guarnieri provided valuable consultations in metal-film deposition procedures. J. M. Karasinski assisted with the formulation and application of the organic coatings, while M. T. Prikas and R. T. White, Jr. assisted in the metal-film depositions. E. Simonyi and M. J. Lysek participated in sample preparation and measurements. Head-fouling tests were carried out by J. Bahr. Useful discussions on the physics of electroerosion were held with J. Bahr, A. J. Lavin, H. Louis, and R. E. McCurry.

References

1. U. Rothgordt, "Document Printing," *Acta Electron.* **21**, 71–82 (1978).
2. R. Reichle, "Information Carrier Construction," U.S. Patent 3,758,336, 1973.
3. D. Atherton, "Electrosensitive Recording Materials," U.S. Patent 3,786,518, 1974.
4. S. Tokumoto and C. Hayashi, "Recording Medium for a Spark Burning Recorder," U.S. Patent 3,861,952, 1975.
5. W. Jung, "Recording Carrier for Electrical Discharge Recording Apparatus," U.S. Patent 4,217,596, 1980.
6. S. Bhatia and R. J. Shuman, "Electrosensitive Recording," U.S. Patent 4,339,758, 1982.
7. A. Suzuki, K. Kubo, S. Kunitake, and F. Arai, "Spark-Recording Type Printing Method and Spark-Recording Material for Use Thereof," U.S. Patent 4,082,902, 1978.
8. M. Figov, A. W. Kent, R. Owen, and P. E. Watts, "Lithographic Printing Plate Preparation," U.S. Patent 4,086,853, 1978.
9. P. Benjamin and C. Weaver, "Measurement of Adhesion of Thin Films," *Proc. Roy. Soc. A* **254**, 163–176 (1960).
10. L. F. Goldstein and T. J. Bertone, "Evaluation of Metal-Film Adhesion to Flexible Substrates," *J. Vac. Sci. Technol.* **12**, 1423–1426 (1975).
11. D. W. Butler, C. T. H. Stoddart, and P. R. Stuart, "The Stylus or Scratch Method for Thin Film Adhesion Measurement: Some Observations and Comments," *J. Phys. D* **3**, 877–883 (1970).
12. B. N. Chapman, "Thin Film Adhesion," *J. Vac. Sci. Technol.* **11**, 106–113 (1974).

13. F. P. Bowden and D. Tabor, *The Friction and Lubrication of Solids*, Vols. 1 and 2, Oxford University Press, London, 1950, 1964.
14. N. I. Polyakov and V. T. Gritsyna, "Determining Critical Load when Testing Adhesion of Metallic Coatings on Solid Bodies," *Zavodskaya Laboratoriya* **43**, 111–112 (1977).
15. H. A. Clark, "Pigment-free Coating Compositions," U.S. Patent 4,027,073.
16. M. S. Nozari, "Abrasion-Resistant Coatings," U.S. Patent 4,049,861.
17. A. Ito, I. Kaetsu, H. Okabo, and M. Kato, "Transparent Resin Composite," U.S. Patent 3,955,035.
18. E. D. Brown, Jr., "Silicone Fluids in Mechanical Applications—A General View," *Proc. Natl. Conf. Fluid Power* **32**, 273–277 (1978).
19. W. E. Campbell, "Solid Lubricants," Chapter 10 in *Boundary Lubrication*, E. F. Ling, E. E. Klaus, and R. S. Fein, Eds., American Society of Mechanical Engineers, New York, 1969.
20. D. Tabor, *The Hardness of Metals*, Oxford University Press, London, 1951.
21. R. Holm, *Electric Contacts*, Springer-Verlag, New York, 1979.
22. F. Llewellyn Jones, *The Physics of Electrical Contacts*, Oxford University Press, London, 1957.
23. L. H. Germer, "The Erosion of Relay Contacts," *Wear* **3**, 188–199 (1960).
24. W. S. Boyle and P. Kisliuk, "Departure from Paschen's Law of Breakdown in Gases," *Phys. Rev.* **97**, 255–259 (1955).
25. P. Kisliuk, "Arcing at Electrical Contacts on Closure. Part V. The Cathode Mechanism of Extremely Short Arcs," *J. Appl. Phys.* **25**, 890–896 (1954).
26. P. Kisliuk, "Electron Emission at High Fields Due to Positive Ions," *J. Appl. Phys.* **30**, 51–55 (1959).
27. L. H. Germer and W. S. Boyle, "Two Distinct Types of Short Arcs," *J. Appl. Phys.* **27**, 32–39 (1956).
28. G. Haase and A. Kleinle, "Zu den kurzen Lichtbögen in elektrischen Kontakten," *Z. angew. Phys.* **18**, 116–120 (1964).
29. E. W. Gray and J. R. Pharney, "Electrode Erosion by Particle Ejection in Low-Current Arcs," *J. Appl. Phys.* **45**, 667–671 (1974).

Received June 29, 1990; accepted for publication July 11, 1991

Mitchell S. Cohen *IBM Research Division, Thomas J. Watson Research Center, P.O. Box 218, Yorktown Heights, New York 10598.* Dr. Cohen received his Ph.D degree from Cornell University, Ithaca, New York. Since joining IBM in 1974, he has worked in the fields of magnetic bubbles and advanced printing technology. Dr. Cohen is currently engaged in research on optoelectronic packaging.

Keith S. Pennington *IBM Research Division, Thomas J. Watson Research Center, P.O. Box 218, Yorktown Heights, New York 10598.* Dr. Pennington graduated with a B.Sc. in physics from Birmingham University, England, in 1957 and a Ph.D. in physics from McMaster University, Hamilton, Ont., Canada, in 1961. He started his research career at Bell Telephone Laboratories, Murray Hill, New Jersey, where he did pioneering work in holography and in particular developed the first multicolor holograms and did early work in holographic interferometry and optical information processing. He joined IBM Research in 1967 and made several leading contributions to the development of improved holographic materials and techniques for three-dimensional scene analysis. Subsequently he initiated the work in and made significant contributions to the development of the Resistive Ribbon Thermal Transfer technology that became the basis for the IBM Quietwriter® printers and other printing programs. Dr. Pennington is Senior Manager of the Image Technologies Department at IBM Research in Yorktown Heights. He currently has responsibility for several image-related research projects in the areas of image compression, document processing, and scanning systems as well as novel high-resolution printing processes. In this position he conceived and managed the development of the dual-function electroNEG materials and formulations for directly producing negatives and lithographic printing masters with the IBM 4250 electroerosion printer. He was awarded the Albert Rose Electronic Imager of the Year Award for 1987 by the Institute for Graphic Communications and the 1987 Charles E. Ives Award for Engineering by the Society of Photographic Scientists and Engineers (SPSE). While at IBM, he has received two Outstanding Contribution Awards, two Outstanding Technical Achievement Awards, and an Outstanding Innovation Award. He has also received a Division Level Award and a Corporate Award for his initiation of the Resistive Ribbon Thermal Transfer printing technology. Dr. Pennington is a Fellow of both the Society for Imaging Science and Technology (IST; formerly SPSE) and the Optical Society of America, a Senior Member of the IEEE, and a member of the Society for Information Display (SID). He is also a member of the Editorial Advisory Board of *Electronic Imaging*.